

On the Classification of 6D SCFTs and Generalized ADE Orbifolds

Jonathan J. Heckman^{1*}, David R. Morrison^{2,3†}, and Cumrun Vafa^{1‡}

¹Jefferson Physical Laboratory, Harvard University, Cambridge, MA 02138, USA

²Department of Mathematics, University of California Santa Barbara, CA 93106, USA

³Department of Physics, University of California Santa Barbara, CA 93106, USA

Abstract

We study $(1, 0)$ and $(2, 0)$ 6D superconformal field theories (SCFTs) that can be constructed in F-theory. Quite surprisingly, all of them involve an orbifold singularity \mathbb{C}^2/Γ with Γ a discrete subgroup of $U(2)$. When Γ is a subgroup of $SU(2)$, all discrete subgroups are allowed, and this leads to the familiar ADE classification of $(2, 0)$ SCFTs. For more general $U(2)$ subgroups, the allowed possibilities for Γ are not arbitrary and are given by certain generalizations of the A- and D-series. These theories should be viewed as the minimal 6D SCFTs. We obtain all other SCFTs by bringing in a number of E-string theories and/or decorating curves in the base by non-minimal gauge algebras. In this way we obtain a vast number of new 6D SCFTs, and we conjecture that our construction provides a full list.

December 2013

*e-mail: jheckman@physics.harvard.edu

†e-mail: drm@physics.ucsb.edu

‡e-mail: vafa@physics.harvard.edu

Contents

1	Introduction	2
2	6D Theories From F-theory	4
3	Building Blocks of 6D SCFTs	8
3.1	(2, 0) Theories	9
3.2	E-String Theory	9
3.3	Single Clusters and Orbifolds	10
3.4	A Plethora of Bases	11
4	Classification of Minimal Models	12
4.1	Algorithm for Minimal Resolutions	14
4.2	No Quartic Vertices	18
4.3	Restrictions on Trivalent Vertices	19
5	Endpoint Classification	22
5.1	Generalized A-Type Theories	24
5.2	Generalized D-Type Theories	26
5.3	Orbifold Examples: A-type theories	27
5.4	Orbifold Examples: D-type theories	28
6	Supplementing a Minimal Model	29
7	Duality Moves	33
8	Conclusions	38
A	Instructions for Using the Mathematica Notebook	40
B	Constraints on Contractible Curve Configurations	40
C	The Gluing Condition in the Maximally Higgsed Case	42
D	Resolution of Orbifold Singularities	44
E	Relevant and Irrelevant Deformations	46
E.1	Multiplicities 6 and 8	47
E.2	Two Blowups Specified	48

1 Introduction

A striking prediction of string compactification is the existence of interacting conformal fixed points in six dimensions. Such theories resist a UV Lagrangian description and involve tensionless strings in the low energy theory.

Theories with $(2, 0)$ supersymmetry in six dimensions admit a simple ADE classification. This is transparently realized by IIB string theory on the background $\mathbb{R}^{5,1} \times \mathbb{C}^2/\Gamma$, with Γ a discrete ADE subgroup of $SU(2)$ [1]. In this description, the tensionless strings of the theory are realized by D3-branes wrapped on collapsing two-cycles of the internal geometry. For the A-series, the dual M-theory description is a stack of coincident M5-branes in flat space [2].

Comparatively far less is known about six-dimensional $(1, 0)$ theories. The most well-known example of this type is the E-string theory, which can be defined as the theory of a small E_8 instanton in heterotic $E_8 \times E_8$ string theory [3–5]. In this description, the E_8 gauge symmetry of the heterotic theory becomes a flavor symmetry of the superconformal theory. Upon further compactification on a T^2 , this provides a realization of the 4D $\mathcal{N} = 2$ Minahan-Nemeschansky theory with E_8 flavor symmetry [6, 7]. Additional examples of $(1, 0)$ theories include the collision of E-type singularities in compactifications of F-theory [8], five-branes placed at ADE singularities [9], and many others [10–18]. However, a systematic classification of $(1, 0)$ theories has not been undertaken.

In this note we classify all possible six-dimensional SCFTs which arise from singular limits of an F-theory compactification. This includes all the previously known examples that we are aware of as well as several new classes of theories. We are therefore led to conjecture that we have the full list.

The basic idea will be to consider F-theory on an elliptically fibered Calabi-Yau threefold $\pi : X \rightarrow B$ over a non-compact complex surface B . Gravity also decouples in such cases. When compact two-cycles of B collapse to zero size, we expect to reach a conformal fixed point with $(1, 0)$ or $(2, 0)$ supersymmetry, signaled by the presence of tensionless strings coming from D3-branes wrapped over the two-cycles. Roughly speaking, the two-cycles of the base B should be viewed as contributing tensionless strings to the 6D theory, while the two-cycles of the fiber contribute massless particles. The combination of the two produces a rich class of possible six-dimensional superconformal field theories.

Some of the previously encountered 6D SCFTs have a simple realization in F-theory. For example, the $(2, 0)$ theories correspond to the special case where the F-theory geometry is $B \times T^2$ with $B = \mathbb{C}^2/\Gamma$ for Γ a discrete subgroup of $SU(2)$. Resolving the base gives a configuration of -2 curves intersecting according to an ADE Dynkin diagram. As another example, the E-string theory corresponds to the generic elliptic Calabi-Yau where the base B is the total space $\mathcal{O}(-1) \rightarrow \mathbb{P}^1$ [19, 20]. The conformal fixed point corresponds to shrinking the base \mathbb{P}^1 to zero size.

An especially important class of six-dimensional SCFTs that we discover are the “minimal” ones with generic elliptic fibration and with no superfluous E-string theories. Quite

surprisingly, this class of SCFTs are all defined by F-theory with base given by an orbifold \mathbb{C}^2/Γ for Γ some discrete subgroup of $U(2)$. Moreover, not all subgroups Γ are allowed. We classify all discrete subgroups consistent with the existence of an elliptic fibration.

To reach this result, we proceed by a process of elimination. Using the classification results on “non-Higgsable” six-dimensional F-theory models [21] and by determining how these non-Higgsable clusters can couple to one another (i.e., their compatibility with the elliptic fibration) we find that the configuration of such curves reduces to an ADE graph consisting of just curves with self-intersection -2 , or a generalized A- or D-type graph of curves where the self-intersection can be less than -2 . Moreover, we show that all such graphs arise as a collection of intersecting \mathbb{P}^1 ’s which blow down to orbifolds of \mathbb{C}^2 , by specific discrete subgroups of $U(2)$. Scanning through all possibilities, we determine the full list of such orbifold singularities.

For the generalized A-type and D-type theories, we find the following infinite families of “rigid” minimal theories:

$$\mathcal{C}_{\text{rigid}}^{(A)} = \alpha A_N \beta \quad \text{for } N \geq 0 \quad (1.1)$$

$$\mathcal{C}_{\text{rigid}}^{(D)} = D_N \gamma \quad \text{for } N \geq 2 \quad (1.2)$$

where A_N and D_N refer to a Dynkin diagram with 2 at each node, and the linear part of the D_N series attaches to γ . Here, α , β and γ are generalized A-type subgraphs of up to five nodes:

$$\alpha \in \{7, 33, 24, 223, 2223, 22223\} \quad (1.3)$$

$$\beta \in \{7, 33, 42, 322, 3222, 32222\} \quad (1.4)$$

$$\gamma \in \{24, 32\}, \quad (1.5)$$

where each label denotes the self-intersection with signs reversed. The rigid theories have the property that increasing the integer at any node would lead to an inconsistent F-theory model. Moreover, by lowering the label to an integer which is at least 2, we reach all the other infinite families of minimal $(1, 0)$ SCFTs. In addition to these infinite families, we also determine all outliers. We find that these only occur in the A-type series for nine or fewer nodes.

Generically, a minimal 6D SCFT can be used to construct non-minimal SCFTs by bringing in additional ingredients: We can bring in a number of E-string theories and/or make the Kodaira-Tate type of the fiber over the curves more singular. This amounts to decorating curves in the base with a self-consistent choice of gauge algebra. Activating a deformation of the gauge algebra then generates a flow to a lower theory. This process can be done for the $(2, 0)$ ADE theories, as well as for many of the other minimal 6D SCFTs. In fact in this way we obtain all the known 6D SCFTs that we are aware of and we conjecture that this construction leads to the full list.

A striking outcome of our analysis is the appearance of discrete subgroups of $U(2)$. Strings on orbifolds of \mathbb{C}^2 which are not strictly contained in $SU(2)$ would lead to a non-supersymmetric compactification, with a closed string tachyon. For work in this direction, see for example [22–27]. The reason we reach a supersymmetric vacuum in our case is that the full F-theory model is still a Calabi-Yau threefold, which generically happens by making the string coupling constant position dependent and of order one. In some very special cases, this arises by embedding the $U(2) \subset SU(3)$ and having the group Γ also act on the elliptic fiber to preserve supersymmetry [19].

The rest of this paper is organized as follows. First, in section 2 we review some relevant aspects of F-theory in six dimensions, and in particular the structure of “non-Higgsable clusters” which appears in the classification of six-dimensional supergravity theories. In section 3 we turn our attention to six-dimensional SCFTs generated by singular limits of F-theory compactifications. Section 4 is the first step in our classification program, where we show that all minimal 6D SCFTs are obtained from ADE type graphs of curves. In section 5 we give the full list of minimal 6D SCFTs. In section 6 we explain in broad terms how to supplement these minimal theories by additional blowups in the base, and more singular behavior in the elliptic fibration. In section 7 we take a top down perspective and explain how to connect various non-minimal SCFTs by duality moves. We present our conclusions in section 8. Some additional mathematical material is collected in a set of Appendices. We also include a brief set of instructions on usage of the `Mathematica` notebook included with the `arXiv` submission.

2 6D Theories From F-theory

To frame our discussion, in this section we review some aspects of F-theory in six dimensions. Since we are dealing with theories with six flat spacetime dimensions and eight real supercharges, we shall be concerned with F-theory compactified on \tilde{X} , a smooth elliptically fibered Calabi-Yau threefold $\tilde{\pi} : \tilde{X} \rightarrow B$ with a section, where B is a complex surface and all of the fibers of $\tilde{\pi}$ have dimension one.¹

Blowing down all fiber components which do not meet the section leads to a singular fibration $\pi : X \rightarrow B$ which always has an equation in Weierstrass form:

$$y^2 = x^3 + fx + g, \tag{2.1}$$

where f and g are sections of the line bundles $\mathcal{O}(-4K_B)$ and $\mathcal{O}(-6K_B)$, respectively. The discriminant locus, which marks where the elliptic fibers are singular, is a section of $\mathcal{O}(-12K_B)$ given by:

$$\Delta = 4f^3 + 27g^2, \tag{2.2}$$

¹If the condition on the fibers is not satisfied, it is possible to blow up the base and possibly perform some flops which gives a new Calabi-Yau threefold satisfying the condition [28].

and should be viewed as indicating the location of seven-branes in the system. If we can reverse the blowdown process, i.e., if the singularities in equation (2.1) can be resolved to a Calabi-Yau threefold \tilde{X} with all fibers one-dimensional, then X determines a nonsingular F-theory model, which is a six-dimensional theory with some number of normalizable tensor multiplets, vector multiplets, and hypermultiplets. Our primary interest is in the class of six-dimensional superconformal field theories we can achieve in these models. For this reason, we shall focus on the case where B is non-compact. This means that a number of the tight restrictions on six-dimensional supergravity theories will not apply. Indeed, this is reflected in the comparative ease with which we will be able to generate various elliptic models.

Each component of the discriminant locus is associated with a seven-brane (or stack of seven-branes) wrapping a curve $\Sigma \subset B$. Each such seven-brane supports a gauge algebra² \mathfrak{g}_Σ which is dictated by the order of vanishing of f , g and Δ along Σ . To obtain a nonsingular F-theory model, along each curve Σ we must either have f vanishing to order less than 4, or g vanishing to order less than 6.³ Higher order vanishing leads to a model with the unfortunate property that on any blowup of X to a smooth space \tilde{X} , the three-form on \tilde{X} always has poles. This strongly suggests such models are unphysical, and they will not be considered here.

The singularities of the elliptic fibration can become worse at the intersection of two components of the discriminant locus; such points are associated with matter fields trapped at the intersection of two seven-branes. An important subtlety here is that to fully specify the field content of the theory, one must start with the smooth Calabi-Yau \tilde{X} and only then take a degeneration limit.⁴

In the maximally Higgsed phase, i.e., after activating all possible hypermultiplet vevs, it is possible to classify the resulting models in terms of the geometry of the base B [21].⁵ In the base geometry, there is a configuration of curves which support seven-brane gauge theories. Such configurations of curves can be decomposed into a set of “non-Higgsable clusters” which only intersect curves with self-intersection -1 .

Let us briefly review this classification result [21]. For a seven-brane wrapping a compact curve Σ , we can analyze the geometry normal to Σ inside of B via its self-intersection. In the maximally Higgsed phase, all possible hypermultiplet vevs are activated. This means, for example, that non-abelian gauge symmetries can only be supported on rigid curves, i.e., ones where the seven-brane cannot move around. Such curves are \mathbb{P}^1 's, with self-intersection $-n < 0$ for some natural number n , and the local geometry is the total space $\mathcal{O}(-n) \rightarrow \mathbb{P}^1$. When $n = 1$ and $n = 2$, one can define a smooth Weierstrass model, i.e., no gauge symmetry

²The global structure of the gauge group is more subtle [29].

³This condition is often stated in a way that includes Δ vanishing to order less than 12, but since $\Delta = 4f^3 + 27g^2$, if f vanishes to order at least 4 and g vanishes to order at least 6, it will automatically be true that Δ vanishes to order at least 12.

⁴For a recent alternative approach which avoids the need to resolve X , see [30]

⁵Note that the analysis of [21] was carried out in the context of a compact base, but the same analysis applies to the case of a neighborhood of a collection of compact curves which we study here.

is present in the maximally Higgsed phase.

When $n > 2$, there is a gauge symmetry, and the *minimal* order of vanishing of f , g and Δ along Σ is dictated by n . The full list of isolated curves which support a gauge symmetry are theories with an \mathfrak{e}_8 seven-brane gauge theory coupled to some number of small instantons, or a seven-brane possibly coupled to a half hypermultiplet. The full list of possibilities is:

7-brane \ cluster	3	4	5	6	7	8	12
\mathfrak{g}_Σ	$\mathfrak{su}(3)$	$\mathfrak{so}(8)$	\mathfrak{f}_4	\mathfrak{e}_6	\mathfrak{e}_7	\mathfrak{e}_7	\mathfrak{e}_8
Hyper	none	none	none	none	$\frac{1}{2}\mathbf{56}$	none	none

(2.3)

where in the second row we have indicated the gauge algebra, and in the third row we have indicated the hypermultiplet content. If we further tune f and g , in general we may obtain higher gauge groups and other matter content which can be Higgsed down to the minimal form above.

For curves of self-intersection -9 , -10 , and -11 , we again find gauge symmetry \mathfrak{e}_8 . However, in these cases there are “small instantons” as well. For example, in the $n = 9$ theory, this is associated with a minimal Weierstrass model:

$$y^2 = x^3 + g_3(z')z^5, \quad (2.4)$$

where z and z' are respectively affine coordinates normal to, and along the curve Σ so that $z = 0$ is the location of the curve Σ , and $g_3(z')$ is a degree three polynomial, and its zeroes specify the locations of “small instantons”. This terminology is borrowed from the heterotic dual description, where it was shown that the \mathbb{P}^1 with self-intersection $-n$ is dual to a strong coupling point of heterotic string theory for maximally Higgsed E_8 with instanton number $12 - n$ [20, 5]. The presence of small instantons means that we do not have a nonsingular F-theory model, but this is repaired by blowing up the base at the location of the zeros of $g_3(z')$, yielding a curve of self-intersection -12 meeting $12 - n$ curves of self-intersection⁶ -1 . When the base is blown up in this way, there is an appropriate modification⁷ of the Weierstrass equation which produces a potentially nonsingular F-theory model. This is our first encounter with the primary issue we must deal with in this paper: determining how much to blow up a given base in order to produce a nonsingular F-theory model.

In addition to isolated curves, there are a few non-Higgsable clusters which have multiple \mathbb{P}^1 's. These configurations are of the form n_1, \dots, n_r , corresponding to \mathbb{P}^1 's with self-intersection $-n_i$ which intersect pairwise at a single point dictated by their location on the

⁶There are other possibilities if the zeroes of $g_3(z')$ have non-trivial multiplicity.

⁷Since the canonical bundle of the blowup base gains an order of vanishing along the -1 curve, the orders of vanishing of f and g along that curve must be reduced by 4 and 6, respectively, by dividing by a power of the local equation of the curve.

string of integers. As found in [21], the full list of such configurations is:

7-brane \ cluster	3, 2	3, 2, 2	2, 3, 2
\mathfrak{g}_Σ	$\mathfrak{g}_2 \oplus \mathfrak{su}(2)$	$\mathfrak{g}_2 \oplus \mathfrak{sp}(1)$	$\mathfrak{su}(2) \oplus \mathfrak{so}(7) \oplus \mathfrak{su}(2)$
Hyper	$\frac{1}{2}(\mathbf{7} + \mathbf{1}, \mathbf{2})$	$\frac{1}{2}(\mathbf{7} + \mathbf{1}, \mathbf{2})$	$\frac{1}{2}(\mathbf{2}, \mathbf{7} + \mathbf{1}, \mathbf{1}) \oplus \frac{1}{2}(\mathbf{1}, \mathbf{7} + \mathbf{1}, \mathbf{2})$

(2.5)

An interesting feature of these clusters is that they contain curves of self-intersection -2 , which support a gauge group factor. This is because these curves intersect another curve which already has a singular fiber, which is then inflicted on its neighbor. Observe that in the 3, 2, 2 configuration, the -3 curve and the middle -2 curve carry gauge symmetry algebras, but the -2 curve at the end does not. We label the symmetry algebra for the middle -2 curve as $\mathfrak{sp}(1)$ rather than $\mathfrak{su}(2)$ because it arises in a different way in F-theory. For additional details, see Appendix C.

Finally, in addition to the non-Higgsable clusters which carry a gauge symmetry, we can also have isolated configurations without a gauge group. These are given by -2 curves which intersect according to an ADE Dynkin diagram.

Now, given a collection of such non-Higgsable clusters, we get a local model for an F-theory base by “gluing” such configurations together using curves of self-intersection -1 . Labelling two such configurations of curves as $\mathcal{C}_{(1)}$ and $\mathcal{C}_{(2)}$, we get a new configuration of curves \mathcal{C}_{new} by introducing an additional -1 curve:

$$\mathcal{C}_{\text{new}} = (\mathcal{C}_{(1)}, 1, \mathcal{C}_{(2)}), \quad (2.6)$$

i.e., we have a -1 curve which intersects a curve $\Sigma_{(1)}$ appearing in the configuration $\mathcal{C}_{(1)}$, and a curve $\Sigma_{(2)}$ appearing in the configuration $\mathcal{C}_{(2)}$.

A priori, there are many ways to piece together such non-Higgsable clusters to form much larger configurations. However, at each stage of gluing, there is a consistency condition which must be satisfied. The two curves $\Sigma_{(1)}$ and $\Sigma_{(2)}$ which we glue via a -1 curve must have appropriate order of vanishing along f , g and Δ to be consistent with having a smooth phase (after resolution). Algebraically, this requires the combined gauge algebra $\mathfrak{g}_{(1)} \oplus \mathfrak{g}_{(2)} \subset \mathfrak{e}_8$ (as we verify in Appendix C). An interesting feature of this condition is that a -6 curve can connect to a -3 curve, provided the -3 curve supports a gauge algebra $\mathfrak{su}(3)$. If, however, the -3 curve supports a \mathfrak{g}_2 gauge algebra (as happens for some NHCs), then the self-intersection must be -5 or more since $\mathfrak{f}_4 \oplus \mathfrak{g}_2$ is a subalgebra of \mathfrak{e}_8 , but $\mathfrak{e}_6 \oplus \mathfrak{g}_2$ is not a subalgebra of \mathfrak{e}_8 .

Finally, if the elliptic fibration is trivial, and only then, it is also possible to add probe five-branes to an F-theory model (otherwise the identity of the five-brane is ambiguous due to $SL(2, \mathbb{Z})$ monodromy), and in addition including the action of orientifolds. This in particular can only be done in the case where we simply have an ADE singularity, and add a number k of D5-branes, with or without orientifold 5-planes, as was studied in [9]. However, as we explain in section 6, this can also be constructed without using five-branes

by considering ADE singularities with additional restrictions on the Kodaira-Tate fiber type over the singularity.

3 Building Blocks of 6D SCFTs

Our interest in this paper concerns the six-dimensional superconformal field theories (SCFTs) generated by singular limits of an F-theory compactification. To reach such SCFTs, we need to take a limit where two-cycles of the base B collapse to zero size. Clearly, the choice of SCFT is dictated by a configuration of smooth curves \mathcal{C} , which we blow down to reach a singular configuration $\mathcal{C}_{\text{sing}}$.

This amounts to a “global” requirement that we can simultaneously contract all of the curves Σ_i of negative self-intersection to zero. Introducing the adjacency matrix:⁸

$$A_{ij} = -(\Sigma_i \cap \Sigma_j), \tag{3.1}$$

this requires A_{ij} to be positive definite, i.e., all eigenvalues must be positive [31–33]. In general, this is a non-trivial condition which excludes many candidate configurations. As an example of an inadmissible configuration, we cannot have two -1 curves intersect, because the adjacency matrix is not positive definite. A related comment is that in any configuration of non-Higgsable clusters, we get a tree-like structure with no closed loops. As explained in Appendix B, there cannot be a physical F-theory model with a loop of contractible curves in the base, for in that case f and g would vanish to orders at least 4 and 6, respectively, along each of the curves in the loop.

From this perspective, the geometric objects of interest are all possible ways that we can arrive at a singular base B which admits *some* resolution to a smooth F-theory model. These different choices of resolution then parameterize different phases of the theory where all states have picked up some tension or mass.⁹ Our task is therefore to classify all the physically distinct SCFTs which arise for some choice of $\mathcal{C}_{\text{sing}}$, and to then determine all possible elliptic fibrations over a given base.

Clearly, there are many choices of non-singular B , so even specifying the full list of bases would at first appear to be a daunting task. As a warmup, in this section we shall therefore discuss some examples of the types of behavior we can expect to encounter. First, we discuss how the $(2, 0)$ theories come about in F-theory. Then, we discuss the case of the E-string theories, which serve as the “glue” joining various non-Higgsable clusters. After this, we turn to the theories defined by a single non-Higgsable cluster. Later, we perform a classification

⁸It is more common to use a central dot to denote the intersection number, which we shall do for the rest of this paper; when the curves are distinct, this means the number of intersection points counted with multiplicity.

⁹In six dimensions, the blowups of the fiber are not part of the Coulomb branch. They are, however, part of the Coulomb branch for the five-dimensional theories defined by a further compactification on a circle.

of all possible 6D SCFTs which can be realized by putting these ingredients together.

3.1 (2, 0) Theories

Let us begin by showing how all the (2, 0) theories come about in our classification. These are specified by a configuration of -2 curves intersecting according to the appropriate ADE Dynkin diagram. The full list consists of two infinite series:

$$A_N : \underbrace{\begin{array}{|c|c|c|} \hline 2 & \dots & 2 \\ \hline \end{array}}_N, \quad D_N : \underbrace{\begin{array}{|c|c|c|c|} \hline & 2 & & \\ \hline 2 & 2 & \dots & 2 \\ \hline \end{array}}_{N-1} \quad (3.2)$$

and the exceptional configurations:

$$E_6 : \begin{array}{|c|c|c|c|c|} \hline & & 2 & & \\ \hline 2 & 2 & 2 & 2 & 2 \\ \hline \end{array}, \quad E_7 : \begin{array}{|c|c|c|c|c|c|} \hline & & 2 & & & \\ \hline 2 & 2 & 2 & 2 & 2 & 2 \\ \hline \end{array}, \quad E_8 : \begin{array}{|c|c|c|c|c|c|c|} \hline & & 2 & & & & \\ \hline 2 & 2 & 2 & 2 & 2 & 2 & 2 \\ \hline \end{array}. \quad (3.3)$$

The special feature of all of these examples is that the base B defines a non-compact Calabi-Yau, i.e., it can be represented as an orbifold \mathbb{C}^2/Γ for Γ discrete subgroup of $SU(2)$. Since the base B is already Calabi-Yau, the elliptic fibration of the model can be trivial, i.e., we can take $B \times T^2$. This means we get theories with (2, 0) supersymmetry. In fact, the ADE classification of such discrete subgroups ensures that this is the full list of (2, 0) theories.

3.2 E-String Theory

Most of the 6D theories we consider will only have eight real supercharges. This means the complex base B will not be Calabi-Yau, and the only way to satisfy the conditions of supersymmetry will be via a non-trivial elliptic fibration. Perhaps the simplest example of this type is the E-string theory defined by the base $\mathcal{O}(-1) \rightarrow \mathbb{P}^1$. We reach the conformal phase by shrinking the \mathbb{P}^1 to zero size.

In some sense, this theory is the “glue” which holds together all of the other (1, 0) theories, so it is worthwhile to discuss it in more detail. One way to arrive at the E-string is to start with the minimal Weierstrass model [34, 20] (see also [3–5, 19]):

$$y^2 = x^3 + z'z^5, \quad (3.4)$$

where (z, z') are coordinates on \mathbb{C}^2 . There is a singularity at the intersection $z' = z = 0$, which is the location of the small instanton. Blowing up the intersection point, we introduce an additional \mathbb{P}^1 , with local geometry $\mathcal{O}(-1) \rightarrow \mathbb{P}^1$. In this geometry, there is a non-compact seven-brane along the locus $z = 0$, corresponding to an E_8 flavor symmetry. Returning to our discussion of gluing NHCs by -1 curves given in section 2 and Appendix C, observe that

we can interpret this gluing construction as gauging a product subalgebra of the \mathfrak{e}_8 flavor symmetry.

There is also a heterotic M-theory dual description of the E-string theory. Starting with a single E_8 wall in flat space, we can introduce an additional M5-brane to probe this theory. The distance of the M5-brane from the wall corresponds to the overall size of the \mathbb{P}^1 . In the limit where the \mathbb{P}^1 shrinks to zero size, the M5-brane touches the wall, and is better viewed as a singular gauge field configuration corresponding to a pointlike instanton.

Now, equation (3.4) is but one presentation of this singular geometry. We can maintain the same singular behavior by including all terms with the same degree along the locus $z = z'$. In the Weierstrass model, this means we can also consider the presentations:

$$y^2 = x^3 + f_4(z, z')x + g_6(z, z'), \quad (3.5)$$

with f_4 and g_6 homogeneous polynomials of respective degrees 4 and 6 in the variables z and z' . As this example makes clear, for some presentations the overall flavor symmetry can be obscured by the choice of equation. However, all of these different choices amount to irrelevant deformations of the 6D theory. We shall return to this point later in section 7, where we take a “top down” perspective on our SCFTs.

3.3 Single Clusters and Orbifolds

The non-Higgsable clusters themselves yield a rich class of $(1, 0)$ theories. Recall that the non-Higgsable clusters contain some configuration of isolated curves which are simultaneously contractible. All of these examples are specified by a linear chain of \mathbb{P}^1 's with negative self-intersection. Though not given this name, some examples of this type were considered in [19].

Upon blowdown, all of these configurations define an orbifold of \mathbb{C}^2 by a discrete cyclic subgroup of $U(2)$. Indeed, a well-known result from the theory of Hirzebruch–Jung resolutions [35–37] is that a configuration of curves:

$$\mathcal{C} = x_1 \cdots x_r \quad (3.6)$$

under blowdown defines the orbifold \mathbb{C}^2/Γ , with Γ a discrete subgroup of $U(2)$ generated by the group action:

$$(z_1, z_2) \mapsto (\omega z_1, \omega^q z_2) \quad \text{where} \quad \omega = e^{2\pi i/p} \quad \text{and} \quad \frac{p}{q} = x_1 - \frac{1}{x_2 - \dots - \frac{1}{x_r}}. \quad (3.7)$$

The specific orbifold for all of the isolated $-n$ theories is:

$$-n \text{ theories: } (z_1, z_2) \mapsto (\omega z_1, \omega z_2) \quad \text{for} \quad \omega = \exp(2\pi i/n), \quad (3.8)$$

while for the clusters with more than one curve, we instead have:

cluster:	3, 2	3, 2, 2	2, 3, 2
p/q	5/2	7/3	8/5

(3.9)

Note that reading the configuration from right to left determines a second generator, which is 5/3 for 3, 2 and 7/5 for 3, 2, 2.

An important feature of these orbifolds is that they are only supersymmetric in the context of F-theory, and not in the more limited context of perturbative IIB string theory. This is because the orbifolds are specified by a $U(2)$ group action which does not embed in $SU(2)$. Nevertheless, supersymmetry is preserved because the profile of the axio-dilaton is non-trivial.

For most of the $-n$ curve theories, the orbifold group action also extends to the elliptic fibration, and we can write the F-theory model as $(\mathbb{C}^2 \times T^2)/\mathbb{Z}_n$. Letting $\lambda = dx/y$ denote the holomorphic differential of the constant T^2 , to get a Calabi-Yau threefold, the holomorphic three-form $dz_1 \wedge dz_2 \wedge \lambda$ must be invariant under the group action, so we have $(z_1, z_2, \lambda) \mapsto (\omega z_1, \omega z_2, \omega^{-2} \lambda)$. For the orbifold to act on the T^2 directions, we also need ω^2 to be of order 1, 2, 3, 4, 6, which in turn means that such a presentation is available for $n = 2, 3, 4, 6, 8, 12$. Observe, however, that the NHCs with $n = 5$ and $n = 7$ are not of this type. For further discussion, see [19].

As a final remark, let us note that the isolated $-n$ curve theories can all be realized in a decoupling limit of F-theory on the Hirzebruch surface \mathbb{F}_n . These complex surfaces are given by a \mathbb{P}^1 bundle over a base \mathbb{P}^1 where the self-intersection of the base is $-n$. For further details of F-theory on Hirzebruch surfaces, see e.g. [19, 34, 20, 38].

3.4 A Plethora of Bases

Clearly, there are a vast number of possible F-theory bases, corresponding to a choice of tree-like structure. For example, it is possible to generate several infinite families of SCFTs by stringing together NHCs into arbitrarily long chains. This includes, for example, some of the chains of NHCs discussed in section 4.3 in [21].

A priori, however, given a chain of NHCs, there is no guarantee that it is possible to simultaneously contract all of the curves in the base. Though rather inefficient, this can be checked on a case by case basis. To illustrate some of these issues, consider the configuration of curves:

$$\mathcal{C} = 313. \tag{3.10}$$

This satisfies the local condition of non-Higgsable clusters, and as can be verified, the adja-

acency matrix:

$$A_{\mathcal{C}} = \begin{bmatrix} 3 & -1 & 0 \\ -1 & 1 & -1 \\ 0 & -1 & 3 \end{bmatrix}, \quad (3.11)$$

is positive definite. However, the seemingly rather similar configuration:

$$\mathcal{C} = 13131 \quad (3.12)$$

does not have a positive definite adjacency matrix. Rather than directly computing the eigenvalues, a more geometric way to see this is to consider the blowdown of the various curves. For a $-n$ curve that abuts a -1 curve, a blowdown of the -1 curve shifts the self-intersection as $n \rightarrow (n - 1)$. Thus, after blowdown we get:

$$\mathcal{C} = 13131 \rightarrow 1221 \rightarrow 11 \rightarrow 0, \quad (3.13)$$

a contradiction.

There is, however, a simple way to arrange a specific class of graphs with a positive definite intersection form: These are given by taking an ADE graph and simply making the self-intersection of a given curve more negative. We will shortly put this observation to use.

4 Classification of Minimal Models

As should now be clear, there is a rich class of 6D SCFTs which can be realized in F-theory. To classify the different possibilities, we need a systematic way to generate SCFTs, and moreover, a way to specify when two singular F-theory geometries yield the same conformal fixed point.

So, suppose we have an F-theory model with some choice of smooth base B . After all resolutions in the base have been performed, we have reached the Coulomb branch of some 6D SCFT. We would like to know which SCFT this is associated with after shrinking all curves in the base to zero size.

As a first step in our classification program, we can consider the related singular geometry obtained by blowing down all -1 curves of the configuration of curves in B . This corresponds to eliminating the blown up -1 curve from the configuration. When we do this, the self-intersection of the remaining curves intersecting each such -1 curve will also shift. For example, if we have a curve Σ of self-intersection $-n$ which intersects the -1 curve E , the class of the curve Σ will shift as:

$$[\Sigma] \rightarrow [\Sigma] + [E] = [\Sigma_{\text{new}}] \quad (4.1)$$

and the self-intersection of $[\Sigma_{\text{new}}]$ is now $-(n-1)$ since:

$$[\Sigma_{\text{new}}] \cdot [\Sigma_{\text{new}}] = [\Sigma] \cdot [\Sigma] + 2[\Sigma] \cdot [E] + [E] \cdot [E] = -(n-1). \quad (4.2)$$

The original configuration of curves \mathcal{C} will therefore blow down to a new configuration \mathcal{C}' . In this new configuration of curves, the process of blowdown may create new -1 curves. Blowing down all of the new -1 curves, and iterating this process, we eventually reach a configuration of curves which contains no -1 curves. We shall refer to this as the “endpoint” of a configuration of curves, $\mathcal{C} \rightarrow \dots \rightarrow \mathcal{C}_{\text{end}}$, and the corresponding base as B_{end} . Examples of such endpoints include the base $B = \mathbb{C}^2$, and the non-Higgsable clusters.

The main result of this section and section 5 will be a classification of *all* such endpoints. We shall refer to the corresponding six-dimensional SCFTs as “minimal” because all of the other F-theory CFTs are obtained by supplementing these theories by additional ingredients such as further blowups and/or by making the elliptic fibration more singular.

Quite surprisingly, it turns out that all the endpoints are specified by taking F-theory on a base of the form:

$$B_{\text{end}} = \mathbb{C}^2/\Gamma, \quad (4.3)$$

where Γ is a discrete subgroup of $U(2)$. For each consistent endpoint, there is a minimal 6D SCFT. The full list of consistent F-theory model bases includes Γ an ADE subgroup of $SU(2)$, as well as specific discrete subgroups of $U(2)$ which we label as

$$A(x_1, \dots, x_r) \quad \text{for} \quad \mathcal{C}_{\text{end}} = x_1 \dots x_r \quad (4.4)$$

$$D(y|x_1, \dots, x_\ell) \quad \text{for} \quad \mathcal{C}_{\text{end}} = \begin{array}{|c|c|c|} \hline & 2 & \\ \hline 2 & y & x_1 \dots x_\ell \\ \hline \end{array} \quad (4.5)$$

The group $A(x_1, \dots, x_r)$ is cyclic of order p with generator acting on the \mathbb{C}^2 coordinates (z_1, z_2) by:

$$(z_1, z_2) \mapsto (\omega z_1, \omega^q z_2), \quad \text{where} \quad \omega = e^{2\pi i/p} \quad \text{and} \quad \frac{p}{q} = x_1 - \frac{1}{x_2 - \dots - \frac{1}{x_r}}. \quad (4.6)$$

The resolution of singularities in this case is a chain $x_1 x_2 \dots x_r$. Note that reading from right to left, i.e. taking the mirror image configuration x_r, \dots, x_1 leads to a different generator of the same orbifold group.

The group $D(y|x_1, \dots, x_\ell)$, on the other hand, is generated by the cyclic group

$$A(x_\ell, \dots, x_1, 2y-2, x_1, \dots, x_\ell) \quad (4.7)$$

and an element Λ of order 4 which sends (z_1, z_2) to $(z_2, -z_1)$:

$$D(y|x_1, \dots, x_\ell) \simeq \langle \Lambda, A(x_\ell, \dots, x_1, 2y-2, x_1, \dots, x_\ell) \rangle. \quad (4.8)$$

As we explain in Appendix D, the resolution of singularities is a chain $y x_1 x_2 \dots x_\ell$ with the

curve of self-intersection $-y$ at the end of the chain meeting two additional curves of self-intersection -2 . The finite subgroups of $U(2)$ have been classified [39–41] and our groups $A(x_1, \dots, x_r)$ and $D(y|x_1, \dots, x_\ell)$ do not exhaust the list, but in addition to the ADE subgroups of $SU(2)$, they are the only ones which occur as endpoints in F-theory.

To reach this result, we shall first show that to be a consistent F-theory model, the topology of any endpoint configuration has the branch structure of an ADE graph, but where the self-intersection of the curves associated with the nodes of the graph can be different from -2 . In particular, we show that if an endpoint contains a curve with self-intersection $-n$ with $n \geq 3$, then the branch structure of the graph is of A- or D-type.

We proceed by assuming that an endpoint exists, and then determine when such endpoints can arise from a blowdown of a configuration of non-Higgsable clusters. If the putative elliptic fibration over the base becomes too singular, we will need to perform some blowups in the base.¹⁰ For a curve of self intersection $-x$ for $x \geq 1$, this will involve blowing up the various intersection points with neighboring curves. Each such blowup shifts the self-intersection of the original curve, so after j blowups, the self-intersection will be $-x^{(j)}$ where:

$$x^{(j)} = x + j. \tag{4.9}$$

On the other hand, since we must be able to resolve the base geometry to some consistent gluing of non-Higgsable clusters, there are upper bounds on how many times a given curve is allowed to be blown up. For example we must have $x^{(j)} \leq 12$.

As we have already mentioned, the first important simplification is that any consistent graph is a tree-like structure, i.e., it contains no closed loops. This is explained in detail in Appendix B. Restricting our analysis to tree-like structures, the remainder of our analysis proceeds in stages. First, we state the general procedure for how to check whether an endpoint can serve as a base for an F-theory model. Then, we whittle away at the possibilities, first by showing that no quartic vertices can exist in an endpoint configuration. Then, we show that there can be at most one trivalent vertex, and that such a vertex can only appear at the end of a graph. This will establish the main claim that all consistent endpoints are given by $U(2)$ orbifolds of \mathbb{C}^2 which form generalizations of the A- and D-type series of Dynkin diagrams. We follow this in section 5 with a list of all consistent endpoints.

4.1 Algorithm for Minimal Resolutions

An important feature of each endpoint is that the intersection pattern dictates a unique minimal resolution of the base geometry. For the ADE series of the $(2, 0)$ theories, no further resolution is required because these are already non-Higgsable clusters. However, the

¹⁰Although we are not discussing Weierstrass equations here, the need to perform blowups can be recognized directly from the equations: any point at which f has multiplicity at least 4 and g has multiplicity at least 6 must be blown up.

seemingly innocuous operation of modifying even a single self-intersection in such a graph can trigger a large set of additional resolutions to reach a base which supports a nonsingular F-theory model. In other words, “hidden between the cracks” of an endpoint configuration are a large set of additional curves.

The main point is that for a given endpoint \mathcal{C}_{end} , there is an algorithm for reaching the uniquely specified minimal resolution:

- I) Check all pairs of nearest neighbors, $x_i x_{i+1}$. If any pairwise intersection occurs which is not on our list of possibilities for a non-Higgsable cluster, we need to blow up the intersection point, i.e., go to $x_i^{(1)} x_{i+1}^{(1)}$. Iterate throughout the entire graph.
- II) Next, check that the gauging condition is satisfied, i.e., that for any pair of curves separated by a -1 curve, that the associated gauge algebra $\mathfrak{g} \oplus \mathfrak{g}' \subset \mathfrak{e}_8$. (The fact that this is the correct condition when the F-theory model is maximally Higgsed is verified geometrically in Appendix C.) If it is satisfied, stop. Otherwise, blowup further.
- III) In such cases, one must always blowup the intersection of the -1 and $-n$ curve for $n > 3$, and for $2 \leq n \leq 3$, it will depend on whether these are part of a non-Higgsable cluster. If they are part of a non-Higgsable cluster, then no blowup is needed. If they are not part of a non-Higgsable cluster, then blowup this intersection point as well.
- IV) Keep repeating until one reaches a configuration of non-Higgsable clusters connected by -1 curves.

In our arXiv submission we also include a `Mathematica` notebook which automates this procedure. See Appendix A for details.

It is helpful to illustrate how to perform such resolutions with some examples (see figure 1 for a depiction). Consider the $(1, 0)$ theory with endpoint:

$$\mathcal{C}_{\text{end}} = 33. \tag{4.10}$$

By inspection, this is not a non-Higgsable cluster, so we need to blowup the intersection point between the two -3 curves. Doing this blowup shifts the self-intersection of the two curves, so we reach:

$$\mathcal{C}_{\text{end}} \rightarrow 414. \tag{4.11}$$

Now, we see that each -4 curve supports an $\mathfrak{so}(8)$ gauge symmetry. We now check the gauging condition at the pair of curves touching our -1 curve. Since $\mathfrak{so}(8) \oplus \mathfrak{so}(8) \subset \mathfrak{e}_8$, we can stop blowing up.

As another example, consider the endpoint configuration:

$$\mathcal{C}_{\text{end}} = 44. \tag{4.12}$$

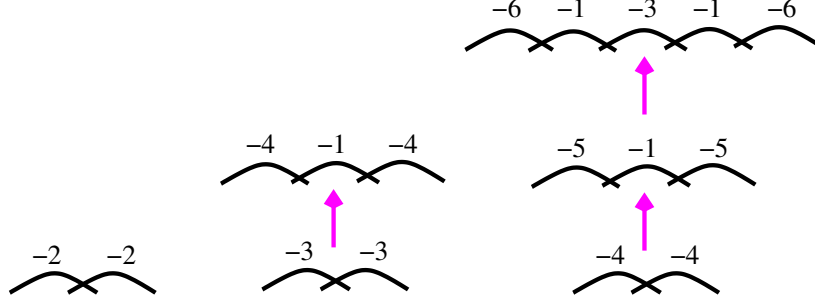


Figure 1: Depiction of the minimal resolution associated with a given endpoint configuration. For a pair of -2 curves which intersect, we have the $(2, 0)$ theory A_2 . For a pair of -3 curves which intersect, a single resolution is required, after which we reach a consistent configuration of non-Higgsable clusters. For a pair of -4 curves, additional resolutions are required. For further discussion of these examples, see lines (4.10)-(4.20).

Following the rules of our algorithm, we first note that this configuration is not a non-Higgsable cluster, so we need to blowup the pair to reach:

$$\mathcal{C}_{\text{end}} \rightarrow 515. \quad (4.13)$$

Now, we check the gauging condition. Here, each -5 curve supports an \mathfrak{f}_4 gauge algebra, so because the product $\mathfrak{f}_4 \oplus \mathfrak{f}_4$ is not contained in \mathfrak{e}_8 , a further blowup is required. In fact, each intersection of the -1 curve with the -5 curve needs to be blown up. First blowup the leftmost -5 curve:

$$\mathcal{C}_{\text{end}} \rightarrow 6125, \quad (4.14)$$

and we see that the sequence 25 is also not a non-Higgsable cluster. So, we need to blowup the intersection between the -2 and -5 curve to reach:

$$\mathcal{C}_{\text{end}} \rightarrow 61316. \quad (4.15)$$

Now we have a set of non-Higgsable clusters, so we again need to check the gauging condition. Here, we have a -6 curve which supports an \mathfrak{e}_6 gauge algebra, and the -3 curve supports an $\mathfrak{su}(3)$ gauge algebra, so we can stop blowing up.

As a final example, consider the endpoint configuration:

$$\mathcal{C}_{\text{end}} = 45. \quad (4.16)$$

Again, the steps are rather similar. We blowup once to reach:

$$\mathcal{C}_{\text{end}} \rightarrow 516. \quad (4.17)$$

Inspection of the clusters yields the minimal algebra $\mathfrak{f}_4 \oplus \mathfrak{e}_6$, which is not a subalgebra of \mathfrak{e}_8 .

So, we need to blowup at the intersection of -5 and -1 , as well as at the intersection of -1 and -6 to reach:

$$\mathcal{C}_{\text{end}} \rightarrow 6126 \rightarrow 61317. \quad (4.18)$$

We cannot stop here, however, because the -7 curve supports an \mathfrak{e}_7 algebra, and the -3 curve supports an $\mathfrak{su}(3)$ algebra, so the product is not a subalgebra of \mathfrak{e}_8 . Following our algorithm, we first attempt blowing up at the intersection of the -1 and -7 curve, so we reach:

$$\mathcal{C}_{\text{end}} \rightarrow 613218. \quad (4.19)$$

Now, the -8 curve supports an \mathfrak{e}_7 algebra, and the -2 curve supports an $\mathfrak{su}(2)$ algebra, so since $\mathfrak{su}(2) \oplus \mathfrak{e}_7 \subset \mathfrak{e}_8$, this satisfies the gauging condition. But we are still not done, because now the pair given by the -6 curve and -3 curve do not satisfy the gauging condition: The -6 curve supports an \mathfrak{e}_6 algebra, while the -3 curve now supports (via the classification of algebras for non-Higgsable clusters) a \mathfrak{g}_2 algebra. So, we must at least blowup the intersection between the -1 curve and the -6 curve. Doing so, we get:

$$\mathcal{C}_{\text{end}} \rightarrow 7123218, \quad (4.20)$$

and as we can verify, this is a configuration of non-Higgsable clusters where the pairwise gauging condition is satisfied. All of the examples on our endpoint list follow the same pattern, and can be worked out by applying the same algorithm.

Let us give some additional more involved examples along these lines. Consider the endpoint configuration of curves:

$$\mathcal{C}_{\text{end}} = 3A_N = \underbrace{32\dots 2}_N. \quad (4.21)$$

For $N \geq 3$, this is not a non-Higgsable cluster, and requires a blowup at the intersection of the -3 and -2 curve. Doing so yields a new configuration:

$$\mathcal{C}_{\text{end}} \rightarrow 413\underbrace{2\dots 2}_{N-1}. \quad (4.22)$$

If $N - 1 = 2$, we can stop blowing up, but if $N - 1 > 2$, then a further set of blowups is required. As a consequence, there is a further cascade of blowups, and we eventually reach the minimal resolution:

$$\mathcal{C}_{\text{end}} \rightarrow \underbrace{41\dots 41}_{N-2}322, \quad (4.23)$$

where in the above, the pattern “41” repeats $N - 2$ times.

Another general feature of our classification is that all of the infinite families mostly consist of -2 curves. The reason for this is that a cascade of blowups rapidly shifts the value of the self-intersection closer to -12 , and this is a strict lower bound which cannot be

violated. To illustrate, consider the endpoint configuration:

$$\mathcal{C}_{\text{end}} = 7A_N7 = \underbrace{72\dots 27}_N, \quad (4.24)$$

for N sufficiently large. After performing all blowups necessary to reach a smooth F-theory model, we reach a configuration with many additional curves:

$$\mathcal{C}_{\text{end}} \rightarrow (12)12231513221(\underbrace{12)122315\dots 513221(12)}_N)12231513221(12), \quad (4.25)$$

where in the end configuration there are $N + 2$ curves with self-intersection -12 , i.e., the N original -2 curves as well as the two -7 curves.

4.2 No Quartic Vertices

We now show that in an endpoint configuration of curves, any given curve can only intersect at most three other curves. To show this, suppose to the contrary, i.e., there is a curve in an endpoint configuration which intersects at least four other curves. First of all, we see that such a graph must contain at least one curve with self-intersection $-n$ for $n \geq 3$. Otherwise, we would have a graph made with just -2 curves, and there is no ADE Dynkin diagram with a quartic vertex.

Now, to reach a non-singular F-theory model, we will need to blowup the various intersection points. Without loss of generality, we can focus on a subgraph such as:

$$\mathcal{C}_{\text{sub}} = \begin{array}{|c|c|c|} \hline & y_1 & \\ \hline y_4 & x & y_2 \\ \hline & y_3 & \\ \hline \end{array}, \quad (4.26)$$

with at least one curve not a -2 curve. Now, this requires us to blowup at least two intersections of x with its neighbors. In fact, once we perform two blowups on x , the self-intersection of this curve is high enough that the other intersection points must also be blown up. By a similar token, this forces even more blowups:

$$\mathcal{C}_{\text{sub}} \rightarrow \begin{array}{|c|c|c|c|c|} \hline & & y_1^{(1)} & & \\ \hline & & 1 & & \\ \hline y_4^{(1)} & 1 & x^{(4)} & 1 & y_2^{(1)} \\ \hline & & 1 & & \\ \hline & & y_3^{(1)} & & \\ \hline \end{array} \rightarrow \begin{array}{|c|c|c|c|c|c|} \hline & & & y_1^{(1)} & & & \\ \hline & & & 2 & & & \\ \hline & & & 1 & & & \\ \hline y_4^{(1)} & 2 & 1 & x^{(8)} & 1 & 2 & y_2^{(1)} \\ \hline & & & 1 & & & \\ \hline & & & 2 & & & \\ \hline & & & y_3^{(1)} & & & \\ \hline \end{array}. \quad (4.27)$$

But now the gauge algebra for $x^{(8)}$ is \mathfrak{e}_8 , so we need four more blowups, so we reach a curve $x^{(12)} > 12$, a contradiction. We therefore conclude that no quartic vertices can appear.

4.3 Restrictions on Trivalent Vertices

In fact, we can also show that in all graphs, there can be at most one trivalent vertex, and aside from the E-type Dynkin diagrams, a trivalent vertex can only appear in a generalized D-type graph.

The analysis proceeds along the same lines as for the exclusion of quartic vertices: We assume the existence of a subgraph, and then perform blowups to attempt to reach a consistent F-theory base consisting of non-Higgsable clusters. If this is not possible, we reach a contradiction.

So to begin, suppose we have a subgraph containing a configuration of curves:

$$\mathcal{C}_{\text{sub}} = \begin{array}{|c|c|c|} \hline & y_1 & \\ \hline y_3 & x & y_2 \\ \hline \end{array} . \quad (4.28)$$

We claim that at least two of the y 's must have self-intersection -2 . That is, the trivalent vertices are of the form:

$$\mathcal{C}_{\text{sub}} = \begin{array}{|c|c|c|} \hline & 2 & \\ \hline 2 & x & y \\ \hline \end{array} . \quad (4.29)$$

To see how this restriction comes about, suppose to the contrary that at least two of the y_i 's have self-intersection -3 or less. Without loss of generality, take them to be y_1 and y_3 . It becomes necessary to blowup all intersections of the x curve with the y curves. Doing so, one reaches the sequence of configurations:

$$\mathcal{C}_{\text{sub}} \rightarrow \begin{array}{|c|c|c|c|c|} \hline & & y_1^{(1)} & & \\ \hline & & 1 & & \\ \hline y_3^{(1)} & 1 & x^{(3)} & 1 & y_2^{(1)} \\ \hline \end{array} \rightarrow \begin{array}{|c|c|c|c|c|c|c|c|} \hline & & & & y_1^{(2)} & & & \\ \hline & & & & 1 & & & \\ \hline & & & & 3 & & & \\ \hline & & & & 1 & & & \\ \hline y_3^{(2)} & 1 & 3 & 1 & x^{(6)} & 1 & 2 & y_2^{(1)} \\ \hline \end{array} . \quad (4.30)$$

Now, at this stage, $x^{(6)} \geq 8$, so the gauge algebra of the x -curve is at least \mathfrak{e}_7 , and the gauging condition with each of the -3 curves is violated. Observe, however, that after even two more blowups, we reach an \mathfrak{e}_8 gauge algebra on the x curve. That means at least five

more blowups must be performed, so we reach the configuration:

$$\mathcal{C}_{\text{sub}} \rightarrow \begin{array}{|c|c|c|c|c|c|c|c|c|c|c|} \hline & & & & & & y_1^{(2)} & & & & \\ \hline & & & & & & 1 & & & & \\ \hline & & & & & & 3 & & & & \\ \hline & & & & & & 2 & & & & \\ \hline & & & & & & 2 & & & & \\ \hline & & & & & & 1 & & & & \\ \hline y_3^{(2)} & 1 & 3 & 2 & 2 & 1 & x^{(11)} & 1 & 2 & 2 & y_2^{(1)} \\ \hline \end{array} . \quad (4.31)$$

This violates the condition $x^{(11)} \leq 12$, a contradiction. In fact, the same sort of argument reveals that the only trivalent vertices which can occur are:

$$\mathcal{C}_{\text{sub}} = \begin{array}{|c|c|c|} \hline & 2 & \\ \hline 2 & 3 & 2 \\ \hline \end{array} \quad \text{or} \quad \begin{array}{|c|c|c|} \hline & 2 & \\ \hline 2 & 2 & y \\ \hline \end{array} , \quad (4.32)$$

where in the former case, this is actually the full endpoint.

We also learn that a trivalent vertex can only appear at the end of a graph, i.e., at most one leg extends to a longer chain. Indeed, suppose to the contrary that y_2 and y_3 of the graph in line (4.28) intersect some other curves with self-intersections $-z_2$ and $-z_3$:

$$\mathcal{C}_{\text{sub}} = \begin{array}{|c|c|c|c|c|} \hline & & y_1 & & \\ \hline z_3 & y_3 & x & y_2 & z_2 \\ \hline \end{array} . \quad (4.33)$$

Since we are assuming that this is not a subgraph in a Dynkin diagram, there will be at least one forced blowup, which will eventually trickle down to our subgraph. Since each additional blowup adds additional constraints, it is enough to demonstrate a contradiction if any of the curves in our subgraph has self intersection $-n$ for $n > 2$.

To this end, we can simply list all possible tree-like subgraphs with low values of the y 's and z 's and check that this never leads to a smooth F-theory model. For example, we have the sequence of forced blowups:

$$\mathcal{C}_{\text{sub}} = \begin{array}{|c|c|c|c|c|} \hline & & 2 & & \\ \hline 3 & 2 & 2 & 2 & 2 \\ \hline \end{array} \rightarrow \dots \rightarrow \begin{array}{|c|c|c|c|c|c|c|c|c|c|c|} \hline & & & & & & & & 3 & & & & \\ \hline & & & & & & & & 2 & & & & \\ \hline & & & & & & & & 2 & & & & \\ \hline & & & & & & & & 1 & & & & \\ \hline 4 & 1 & 5 & 1 & 3 & 2 & 2 & 1 & (12) & 1 & 2 & 2 & 3 & 2 \\ \hline \end{array} , \quad (4.34)$$

which eventually leads to a contradiction. The other case to cover is:

$$\mathcal{C}_{\text{sub}} = \begin{array}{|c|c|c|c|c|} \hline & & 3 & & \\ \hline 2 & 2 & 2 & 2 & 2 \\ \hline \end{array} \rightarrow \dots \rightarrow \begin{array}{|c|c|c|c|c|c|c|c|c|c|} \hline & & & & 5 & & & & & & \\ \hline & & & & 1 & & & & & & \\ \hline & & & & 3 & & & & & & \\ \hline & & & & 2 & & & & & & \\ \hline & & & & 2 & & & & & & \\ \hline & & & & 1 & & & & & & \\ \hline 2 & 3 & 2 & 2 & 1 & (12) & 1 & 2 & 2 & 3 & 2 \\ \hline \end{array}, \quad (4.35)$$

which also leads to an inconsistent model. Putting a -3 curve further into the interior only makes the putative elliptic fibration more singular.

As a result of these limitations on trivalent vertices, we can also see that the short legs of the trivalent vertices must be -2 curves. Otherwise, we will inflict too many blowups on the subgraph. For example, we reach a contradiction for the configuration:

$$\mathcal{C}_{\text{sub}} = \begin{array}{|c|c|c|c|} \hline & 3 & & \\ \hline 2 & 2 & 2 & 2 \\ \hline \end{array} \rightarrow \dots \rightarrow \begin{array}{|c|c|c|c|c|c|c|c|c|c|} \hline & & & & 5 & & & & & & \\ \hline & & & & 1 & & & & & & \\ \hline & & & & 3 & & & & & & \\ \hline & & & & 2 & & & & & & \\ \hline & & & & 2 & & & & & & \\ \hline & & & & 1 & & & & & & \\ \hline 3 & 2 & 2 & 1 & (12) & 1 & 2 & 2 & 3 & 2 \\ \hline \end{array}, \quad (4.36)$$

which also leads to an inconsistent model.

Hence, if a trivalent vertex appears in an endpoint, then it must appear as part of a graph:

$$\mathcal{C}_{\text{sub}} = \begin{array}{|c|c|c|c|} \hline & 2 & & \\ \hline 2 & 2 & y_1 & \dots \\ \hline \end{array}, \quad (4.37)$$

where nothing else intersects the -2 curves on the legs of the vertex. Due to this limitation, we have already placed a strong restriction on endpoints: There can be at most two trivalent vertices, and these can only appear at the ends of a linear chain of curves.

In fact, there can be at most one trivalent vertex in an endpoint configuration. Suppose to the contrary that we have a configuration of curves with two trivalent vertices:

$$\mathcal{C}_{\text{end}} = \begin{array}{|c|c|c|c|c|c|c|} \hline & 2 & & & & 2 & \\ \hline 2 & 2 & y_1 & \dots & y_r & 2 & 2 \\ \hline \end{array}, \quad (4.38)$$

where $r \geq 1$. We must have at least one curve with self-intersection less than -2 , since the Dynkin diagram classification contains no graphs with two trivalent vertices. By inspection, each pairwise intersection of curves must be blown up at least once. This means we reach

the configuration:

$$\mathcal{C}_{\text{end}} \rightarrow \begin{array}{|c|c|c|c|c|c|c|c|c|c|c|} \hline & 2 & & & & & & & & 2 & \\ \hline 2 & 3 & 1 & y_1^{(2)} & 1 & \dots & 1 & y_r^{(2)} & 1 & 3 & 2 \\ \hline \end{array} . \quad (4.39)$$

Because the -3 curves in each trivalent vertex sit in the middle of an NHC, each supports an $\mathfrak{so}(7)$ gauge algebra. Since $\mathfrak{so}(7) \oplus \mathfrak{f}_4$ is not a subalgebra of \mathfrak{e}_8 we see that if $y_1^{(2)} \geq 3$, a further set of blowups will be generated. For example, if $y_1^{(2)} \geq 3$, then, there are some forced blowups:

$$\mathcal{C}_{\text{end}} \rightarrow \begin{array}{|c|c|c|c|c|c|c|c|c|c|c|} \hline & 2 & & & & & & & & 2 & \\ \hline 2 & 3 & 1 & y_1^{(2)} & 1 & \dots & 1 & y_r^{(2)} & 1 & 3 & 2 \\ \hline \end{array} \quad (4.40)$$

$$\rightarrow \begin{array}{|c|c|c|c|c|c|c|c|c|c|c|} \hline & 2 & & & & & & & & & 2 \\ \hline 2 & 4 & 1 & 3 & 1 & y_1^{(3)} & 1 & \dots & 1 & y_r^{(2)} & 1 & 3 & 2 \\ \hline \end{array} \quad (4.41)$$

$$\rightarrow \begin{array}{|c|c|c|c|c|c|c|c|c|c|c|c|} \hline & & 3 & & & & & & & & & & \\ \hline & & 1 & & & & & & & & & 2 & \\ \hline 3 & 1 & 6 & 1 & 3 & 1 & y_1^{(3)} & 1 & \dots & 1 & y_r^{(2)} & 1 & 3 & 2 \\ \hline \end{array} . \quad (4.42)$$

Owing to the trivalent vertex on the righthand side, we now reach a contradiction. The reason is that at least one more blowup on y_1 is required, and this sets off a cascade on the leftmost vertex.

Based on this, we conclude that $y_1 = y_r = 2$. In fact, the same reasoning applies for all of the interior curves, so we require $y_i = 2$ for all i . In other words, the only option left is an affine D-type Dynkin diagram. This, however, contradicts the original requirement that we can simultaneously contract all curves to zero size. We therefore conclude that at most one trivalent vertex can appear in a graph.

5 Endpoint Classification

In this section we present the results of our classification of endpoints. There are two steps to this procedure. First, we identify candidate endpoint configurations consisting of generalized A- or D-type graphs. Then, we perform a minimal resolution according to the algorithm detailed in subsection 4.1 (see also Appendix A). Provided we reach a set of non-Higgsable clusters, we admit this endpoint. Otherwise, we reject it. The plan is simply to sweep over all possible endpoint configurations using an automated program.

In fact, it is “only” necessary to scan configurations with ten curves or less. The reason is that starting at eleven curves, the innermost curves of an endpoint are always -2 curves. This means that any candidate patterns found at ten curves can either continue to a string of eleven or more curves, or go extinct. These patterns are given by five curves on the left of a graph, and five on the right, with a string of -2 curves in the middle.

To see how this comes about, suppose we have a subgraph of the form:

$$\mathcal{C}_{\text{sub}} = x_1x_2x_3x_4x_5x_6x_7x_8x_9x_{10}x_{11}. \quad (5.1)$$

In this case, the claim is that $x_6 = 2$. Indeed, suppose to the contrary. Then, we have the sequence of forced blowups:

$$\mathcal{C}_{\text{sub}} \rightarrow x_1x_2x_3^{(1)}1x_4^{(2)}1x_5^{(2)}1x_6^{(2)}1x_7^{(2)}1x_8^{(2)}1x_9^{(1)}x_{10}x_{11} \quad (5.2)$$

$$\rightarrow x_1x_2x_3^{(1)}1x_4^{(3)}131x_5^{(4)}131x_6^{(4)}131x_7^{(4)}131x_8^{(3)}1x_9^{(1)}x_{10}x_{11} \quad (5.3)$$

$$\rightarrow x_1x_2x_3^{(1)}1x_4^{(3)}131x_5^{(4)}13221x_6^{(8)}12231x_7^{(4)}131x_8^{(3)}1x_9^{(1)}x_{10}x_{11} \quad (5.4)$$

$$\rightarrow x_1x_2x_3^{(1)}1x_4^{(3)}131x_5^{(5)}131513221x_6^{(10)}122315131x_7^{(5)}131x_8^{(3)}1x_9^{(1)}x_{10}x_{11}, \quad (5.5)$$

so for $x_6 > 2$ we generate a contradiction. This means that starting at eleven or more curves, the only configurations are:

$$\mathcal{C}_{\text{sub}} = x_1x_2x_3x_4x_5 \underbrace{2 \dots 2}_N y_5y_4y_3y_2y_1. \quad (5.6)$$

Thus, classification requires us to determine all consistent x_i and y_j .

There are some additional simplifications which help in reducing the time of the computation. For two or more curves, the value of x for a curve of self-intersection $-x$ is bounded as $2 \leq x \leq 9$. Moreover, the deeper we go into the interior of a graph, the tighter the upper bound on x .

Rather than listing all of the different endpoints, we only give the ones which are ‘‘rigid’’ in the sense that any further increase in the value of x for a curve of self-intersection $-x$ would produce an inconsistent endpoint. Since decreasing the value of x also produces a consistent endpoint¹¹ (provided the new value is greater than or equal to two), this collection of theories forms a convex hull, and our task is to determine its shape.

For the A-type and D-type theories, we find the following infinite rigid families:

$$\mathcal{C}_{\text{rigid}}^{(A)} = \alpha A_N \beta \quad \text{for } N \geq 0 \quad (5.7)$$

$$\mathcal{C}_{\text{rigid}}^{(D)} = D_N \gamma \quad \text{for } N \geq 2 \quad (5.8)$$

where A_N and D_N refer to a configuration of -2 curves, which are decorated on the end by

¹¹This is because a -1 curve can meet the curve of self-intersection $-x$ in a larger configuration, and blowing that -1 curve down yields a configuration in which x has been decreased by 1.

configurations α , β and γ of up to five curves:

$$\alpha \in \{7, 33, 24, 223, 2223, 22223\} \quad (5.9)$$

$$\beta \in \{7, 33, 42, 322, 3222, 32222\} \quad (5.10)$$

$$\gamma \in \{24, 32\}. \quad (5.11)$$

This is the complete list of rigid theories for ten or more curves. In addition to these infinite families, there are some outlier rigid theories for the A-type graphs which occur at nine or fewer curves:

$$\mathcal{C}_{\text{rigid outliers}}^{(A)} \in \left\{ \begin{array}{l} (12), 92, 83, 822, 8222, 82222, \\ 352, 343, 262, 2522, 25222, 252222, \\ 22422, 224222, 2242222, 2224222, 22242222, 222242222 \end{array} \right\}. \quad (5.12)$$

In the above list, the configuration (12) refers to a single curve of self-intersection -12 . The mirror image configurations of curves define a different generator of the same orbifold group.

In the rest of this section we give more details of performing such a sweep. First, we give the generalized A-type graphs, and then the generalized D-type graphs. We then discuss the characterization of some of these theories in terms of their associated orbifold group action.

5.1 Generalized A-Type Theories

We begin with A-type graphs of the form:

$$\mathcal{C}_{\text{end}} = x_1 \dots x_r. \quad (5.13)$$

There is a built in symmetry here due to the fact that the word $x_r \dots x_1$ specifies the same geometry. We shall therefore only give one representative in our endpoint list, sorting lexicographically according to larger values of x_1 first. There are some clear patterns which either go extinct, or continue on to an arbitrary number of curves. For the list of rigid A-type theories with up to ten curves, see table 1.

At this point, we can identify the general patterns which persist to an arbitrary number of curves:

$$\mathcal{C}_{\text{rigid}}^{(A)} = \alpha A_N \beta \quad \text{for } N \geq 0 \quad (5.14)$$

where α and β are configurations of up to five curves in the set:

$$\alpha \in \{7, 33, 24, 223, 2223, 22223\} \quad (5.15)$$

$$\beta \in \{7, 33, 42, 322, 3222, 32222\}. \quad (5.16)$$

Additionally, table 1 contains all outlier cases for nine or fewer curves.

1	2	3	4	5	6	7	8	9	10
(12)									
	92								
	83	822	8222	82222					
	77	742	7322	73222	732222				
		733	7233	72322	723222	7232222			
		727	7242	72242	722322	7223222	72232222	722232222	7222232222
		352	7227	72233	722242	7222322	72223222	722223222	7222223222
		343	3422	72227	722233	7222242	72222322	722222322	7222222322
		262	3342	34222	722227	7222233	72222242	722222242	7222222242
			3333	33322	342222	7222227	72222233	722222233	7222222233
			2522	33242	333222	3332222	72222227	722222227	7222222227
			2442	33233	332322	3323222	33232222	332232222	3322232222
				32322	332242	3322322	33223222	332223222	3322223222
				32242	332233	3322242	33222322	332222322	3322222322
				25222	252222	3322233	33222242	332222242	3322222242
				24322	243222	2432222	33222233	332222233	3322222233
				24242	242322	2423222	24232222	242232222	2422232222
				22422	242242	2422322	24223222	242223222	2422223222
					242233	2422242	24222322	242222322	2422222322
					224222	2242222	24222242	242222242	2422222242
					223322	2233222	23232222	232232222	2322232222
						2232322	23223222	232223222	2322223222
						2224222	23222322	232222322	2322222322
							22332222	223232222	2232232222
							22323222	223223222	2232223222
							22322322	223222322	2232222322
							22242222	222332222	2223232222
							22233222	222242222	2222332222

Table 1: Table of rigid theories for A-type graphs for up to ten curves. The first row indicates the number of curves, and all subsequent rows indicate the specific endpoint configuration. In the first column, (12) refers to a single curve of self-intersection -12 . In all other cases, the self-intersection of the curves is $-x$ for $2 \leq x \leq 9$. As the number of curves increases, some patterns either go extinct, or persist to an arbitrary number of curves.

5.2 Generalized D-Type Theories

In the case of the D-type theories, we can perform a similar sweep. Due to the presence of a trivalent vertex in D-type graphs, far fewer cases need to be considered. For example, at four curves, we have the rigid configurations:

$$\mathcal{C}_{\text{rigid}} = \begin{array}{|c|c|c|} \hline & 2 & \\ \hline 2 & 3 & 2 \\ \hline \end{array}, \quad \begin{array}{|c|c|c|} \hline & 2 & \\ \hline 2 & 2 & 4 \\ \hline \end{array}. \quad (5.17)$$

The minimal resolution for these two cases is:

$$\begin{array}{|c|c|c|} \hline & 2 & \\ \hline 2 & 3 & 2 \\ \hline \end{array} \rightarrow \begin{array}{|c|c|c|c|c|} \hline & & 3 & & \\ \hline & & 1 & & \\ \hline 3 & 1 & 6 & 1 & 3 \\ \hline \end{array}. \quad (5.18)$$

and:

$$\begin{array}{|c|c|c|} \hline & 2 & \\ \hline 2 & 2 & 4 \\ \hline \end{array} \rightarrow \begin{array}{|c|c|c|c|} \hline & 2 & & \\ \hline 2 & 3 & 1 & 5 \\ \hline \end{array} \rightarrow \begin{array}{|c|c|c|c|c|c|c|} \hline & & 3 & & & & \\ \hline & & 1 & & & & \\ \hline 3 & 1 & 6 & 1 & 3 & 1 & 6 \\ \hline \end{array}. \quad (5.19)$$

The reason for the second blowup is that the -5 curve abuts a -3 curve in the middle of a non-Higgsable cluster, so the algebra is $\mathfrak{f}_4 \oplus \mathfrak{so}(7)$, which is not a subalgebra of \mathfrak{e}_8 . Compared with the A-type graphs, this is the reason such graphs produce far fewer rigid theories. In the minimal resolutions of the A-type graphs, a -3 curve which abuts a -5 curve yields a \mathfrak{g}_2 algebra, and $\mathfrak{f}_4 \oplus \mathfrak{g}_2$ is a subalgebra of \mathfrak{e}_8 .

At five curves and above, all of the graphs have the general form:

$$\mathcal{C}_{\text{end}} = \begin{array}{|c|c|c|} \hline & 2 & \\ \hline 2 & 2 & x_1 \dots x_r \\ \hline \end{array}. \quad (5.20)$$

In fact, we can simply repurpose our classification results for A-type graphs for this case as well. Owing to the trivalent vertex, we cannot tolerate many blowups in its vicinity. For rigid D-type theories, we find no outliers, and all are of one of two types:

$$\mathcal{C}_{\text{rigid}}^{(D)} = D_N \gamma \quad \text{for } N \geq 2, \quad (5.21)$$

where γ is a configuration of curves in the set:

$$\gamma \in \{32, 24\}. \quad (5.22)$$

	22227	22233	22242	22322	23222	32222
72222	$\frac{36N+336}{6N+55}$	$\frac{30N+264}{5N+43}$	$\frac{30N+257}{5N+42}$	$\frac{24N+190}{4N+31}$	$\frac{30N+209}{5N+34}$	$\frac{36N+216}{6N+35}$
33222		$\frac{25N+205}{10N+81}$	$\frac{25N+200}{10N+79}$	$\frac{20N+147}{8N+58}$	$\frac{25N+160}{10N+63}$	$\frac{30N+163}{12N+64}$
24222			$\frac{25N+195}{15N+116}$	$\frac{20N+143}{12N+85}$	$\frac{25N+155}{15N+92}$	$\frac{30N+157}{18N+93}$
22322				$\frac{16N+104}{12N+77}$	$\frac{20N+111}{15N+82}$	$\frac{24N+110}{18N+81}$
22232					$\frac{25N+115}{20N+91}$	$\frac{30N+109}{24N+86}$
22223						$\frac{36N+96}{30N+79}$

Table 2: Table of values for the fraction $p/q = x_1 - \frac{1}{x_2 - \dots - \frac{1}{x_r}}$ for the 21 physically distinct rigid endpoint configurations at ten or more curves. All of these configurations are of the form $\alpha A_N \beta$ for appropriate α and β a configuration of five curves indicated in the highest row and leftmost column. The orbifold group action is $(z_1, z_2) \mapsto (\omega z_1, \omega^q z_2)$ for ω a primitive p^{th} root of unity. By reversing the order of the curves in the graph, we would get a different generator of the orbifold group action which is geometrically identical.

5.3 Orbifold Examples: A-type theories

Since we now have a list of the various endpoints, we can also determine the explicit form of the orbifold group action. In this subsection, we focus on some of the A-type theories.

Recall that for an A-type graph of curves $x_1 \dots x_r$, we have the orbifold group action $A(x_1, \dots, x_r)$:

$$(z_1, z_2) \mapsto (\omega z_1, \omega^q z_2) \quad \text{where} \quad \omega = e^{2\pi i/p} \quad \text{and} \quad \frac{p}{q} = x_1 - \frac{1}{x_2 - \dots - \frac{1}{x_r}}. \quad (5.23)$$

In table 2 we collect the values of p/q for all rigid configurations of ten or more curves.

Consider next the $x A_N y$ theories for $2 \leq x, y \leq 7$. The orbifold generated by the $1/p$ and q/p roots of unity is:

$$\frac{1}{p} = \frac{1}{N(x-1)(y-1) + xy - 1} \quad \text{and} \quad \frac{q}{p} = \frac{N(y-1) + y}{N(x-1)(y-1) + xy - 1}. \quad (5.24)$$

An interesting feature of this example is that at least for some of the rigid theories with $x = y = 7$, there is a simple realization of the F-theory model as an orbifold $(\mathbb{C}^2 \times T^2)/\Gamma$:

$$\Gamma : (z_1, z_2, \lambda) \mapsto (\eta \zeta^{-1} z_1, \eta \zeta z_2, \eta^{-2} \lambda), \quad (5.25)$$

where the group action in the base $(z_1, z_2) \mapsto (\eta\zeta^{-1}z_1, \eta\zeta z_2)$ is by an A-type orbifold. For example, consider

$$\eta = \exp\left(2\pi i \cdot \frac{1}{12}\right) \quad \text{and} \quad \zeta = \exp\left(2\pi i \cdot \frac{k}{12k+1}\right). \quad (5.26)$$

The base of the F-theory model is an A-type $U(2)$ orbifold of \mathbb{C}^2 with values of $1/p$ and q/p :

$$\frac{1}{p} = \frac{1}{12(12k+1)} \quad \text{and} \quad \frac{q}{p} = \frac{24k+1}{12(12k+1)}, \quad (5.27)$$

which matches to our general expression in line (5.24) for $N = 4k - 1$ and $x = y = 7$.

Finally, as a brief aside, let us note that one can also generate F-theory models on $(\mathbb{C}^2 \times T^2)/\Gamma$ by combining an ADE orbifold of \mathbb{C}^2 with a \mathbb{Z}_n orbifold of the T^2 :

$$\Gamma : (z_1, z_2, \lambda) \mapsto (\alpha\rho_1(z_1, z_2), \alpha\rho_2(z_1, z_2), \alpha^{-2}\lambda), \quad (5.28)$$

where α^2 is of order 1, 2, 3, 4, 6. Here, ρ_i denotes the group action on the z_i coordinate and λ is the holomorphic differential of a constant T^2 . The special case where the ADE subgroup is trivial corresponds to the class of examples reviewed in subsection 3.3.

A priori, however, there is no guarantee that such orbifold actions correspond to endpoint theories. Rather, they could involve supplementing an endpoint theory by additional blowups or higher singularities in the elliptic fiber, as well as non-isolated singularities (non-compact flavor seven-branes). Additionally, as we already saw in subsection 3.3, not all endpoint theories have such a simple elliptic fibration. Indeed, not even all rigid theories can be represented as orbifolds. For example $\mathcal{C}_{end} = 92$ involves a \mathbb{Z}_{17} orbifold in the base.

5.4 Orbifold Examples: D-type theories

The group actions and resolutions for D-type theories do not seem to be in the literature in an explicit form, so we describe them in Appendix D. As mentioned earlier, we start with a cyclic group action, specified by a fraction p/q , and then we supplement that with an additional group generator $(z_1, z_2) \mapsto (z_2, -z_1)$.

The rigid endpoint $D_N 24$ corresponds to the fraction

$$\frac{p}{q} = \frac{18N - 12}{6N - 5} \quad (5.29)$$

while the rigid endpoint $D_N 32$ corresponds to the fraction

$$\frac{p}{q} = \frac{18N - 24}{12N - 17}. \quad (5.30)$$

We have also calculated the fraction for the endpoint $D_N 23$, which is the only non-ADE graph which can be obtained from a rigid endpoint by lowering one or more x 's. The fraction is

$$\frac{p}{q} = \frac{8N - 4}{4N - 3}. \quad (5.31)$$

6 Supplementing a Minimal Model

Our focus up to this point has been on a classification of endpoints. In this section we discuss the various ways to go beyond these minimal cases. Recall that starting from an endpoint, there is a unique way to perform a minimal resolution, and there is also a minimum order of vanishing for f , g and Δ for the Weierstrass model. With enough foresight, instead of specifying a minimal resolution, one could instead simply list the specific order of vanishing for f , g and Δ on each of the curves of an endpoint configuration.

Now, it is sometimes possible to make the Kodaira-Tate fiber more singular on a given curve, i.e., by increasing the order of vanishing of f , g and Δ over a given curve. This should be viewed as giving another SCFT which upon smoothing can flow back down to one of our endpoint configurations. In the blown up phase, this smoothing can be interpreted as a Higgs mechanism for the seven-brane gauge theory.

To unambiguously assign a CFT to a given F-theory model, we therefore need to give a configuration of curves, and then also specify the gauge algebra over the curves and intersection points.¹² This sort of supplementing leads us to new $(1, 0)$ theories, and can be done for all of the ADE $(2, 0)$ theories, as well as many of the minimal $(1, 0)$ SCFTs found in section 5.

As we just mentioned, one way to supplement a theory involves decorating the curves of an endpoint configuration by a gauge algebra of higher rank than the minimal one required to define an elliptic model. For example, in the A-type $(2, 0)$ theory given by a configuration of -2 curves, we can either leave the curves undecorated, or make the elliptic fiber more

¹²Recently it has been found that a singular compactification of F-theory can contain various ambiguities, which are repaired by including additional T-brane data [42] (see also [43–45]). The important point for our considerations is that non-trivial T-brane data corresponds to moving onto the Higgs branch of a putative 6D SCFT, i.e., it introduces a mass scale through the presence of a seven-brane flux and non-trivial Higgs field profile.

For our present purposes, such phenomena should be viewed as specifying a Higgs branch for the moduli space of a six-dimensional theory which already has a geometric description. This can in principle lead to a new flow, but the IR fixed point is still characterized by the gauge algebra on the configuration of curves. Additionally, we do not expect to reach any isolated 6D SCFTs which are completely disconnected from a geometric realization.

In four-dimensional SCFTs, T-brane data instead shows up as a mass deformation of the CFT realized on the worldvolume of a D3-brane probing a stack of seven-branes (see e.g. [46–49]).

singular by decorating each curve by the same gauge algebra:

$$\mathcal{C}_{\text{generic}} = \underbrace{2 \quad \dots \quad 2}_N \quad \text{versus} \quad \mathcal{C}_{\text{tuned}} = \underbrace{\mathfrak{su}(m) \quad \dots \quad \mathfrak{su}(m)}_N, \quad (6.1)$$

where by abuse of notation, we refer to the singularity type according to the gauge symmetry it would generate in the resolved phase. This can be done for any of the $(2, 0)$ ADE theories, and gives a purely geometric realization of the $(1, 0)$ theories of [9] obtained from five-branes probing an ADE singularity. Note that if the Kodaira-Tate fiber is more singular than the generic model with a given base, then the gluing condition will not involve a product algebra inside of \mathfrak{e}_8 . Rather, it will involve a product contained in a parent simple gauge algebra. For example, a -1 curve can meet two curves carrying $\mathfrak{so}(m)$ and $\mathfrak{so}(n)$ gauge symmetry for arbitrary values of m and n , and $\mathfrak{so}(m) \oplus \mathfrak{so}(n) \subset \mathfrak{so}(m+n)$ [50, 8]. In general, once we go above the minimal singular behavior for an elliptic fibration, there are additional consistency conditions for gluing besides embedding a product in a simple parent algebra.

It is also sometimes possible to introduce other singular fibers, such as the II^* fiber associated with an \mathfrak{e}_8 gauge algebra. In such cases, additional blowups in the base are generically required. A class of examples covered in this way includes small instantons of heterotic theory on top of an ADE singularity of a K3 surface [16]. Under heterotic/F-theory duality, the ADE singularity of the heterotic theory becomes a stack of strongly coupled seven-branes with ADE gauge group. Introducing additional pointlike instantons corresponds to further blowups of the base geometry. Performing such blowups, we generically make the singularity type worse, which in turn can require even more blowups.

Specifying a non-minimal theory amounts to introducing extra blowups in the base, and decorating it with a consistent choice of gauge algebras.¹³ These two steps are typically interrelated. First, we can enlarge the class of possible bases by introducing non-minimal blowups of an endpoint. Physically, this corresponds to incorporating additional E-string theories. For each such base, there is a minimal order of vanishing for f , g , and Δ for each contractible curve, which can be shifted up by introducing extra blowups. Additionally, for a given base, we can decorate each curve with a higher rank gauge algebra. This will in general violate a gluing/gauging condition, so further blowups in the base will then be required. Once we go beyond the minimal Kodaira-Tate type for the elliptic fiber, there are also extra compatibility conditions besides just “fitting inside a parent simple gauge algebra”. It would be interesting to work out these conditions in full generality. Finally, activating a deformation by giving a vev to an operator in the SCFT can then induce flows to lower theories.

Let us illustrate how blowing up can shift the minimal singularity type of the elliptic

¹³Note that decorating by the choice of gauge algebra rather than just the Kodaira-Tate fiber allows us to also cover T-brane deformations of the F-theory model.

fibration. The most trivial example is to start with F-theory on the base $B = \mathbb{C}^2$. Blowing up once, we get a single -1 curve, which is the E-string theory. Blowing up again, we get the configuration $\mathcal{C} = 12$. Blowing up again, we can either reach the theory 122 or 131, or 213. If we now blow down the -1 curve in the last two theories, we get a theory $\mathcal{C} = 12$, but where the -2 curves supports a gauge algebra. This can be deformed down to the generic case where the -2 curve has a smooth elliptic fiber. We return to this example in section 7.

As a more involved example, consider next the endpoint configuration and its minimal resolution:

$$\mathcal{C}_{\text{end}} = 33, \text{ and } \mathcal{C}_{\text{min}} = 414 = \begin{array}{c} \mathfrak{so}(8) \quad \mathfrak{so}(8) \\ 4 \quad 1 \quad 4 \end{array}, \quad (6.2)$$

where we have indicated the minimal singularity type. Now, we can choose to perform some further blowups, and doing so leads us to a new theory. For example, an additional blowup on the -4 curve on the right takes us to:

$$\mathcal{C}_{\text{n-min}} \rightarrow 4151. \quad (6.3)$$

We cannot stop here, however, because our non-Higgsable clusters now violate the local gauging condition for nearest neighbors! We therefore need to go through the same steps we did for the endpoints, now for this non-minimal case. The process terminates after one further blowup:

$$\mathcal{C}_{\text{min}} \rightarrow 513161 = \begin{array}{c} \mathfrak{f}_4 \quad \mathfrak{su}(3) \quad \mathfrak{e}_6 \\ 5 \quad 1 \quad 3 \quad 1 \quad 6 \quad 1 \end{array}, \quad (6.4)$$

which satisfies the gauging condition. Observe that by a further tuning, we can supplement \mathfrak{f}_4 to convert it to an \mathfrak{e}_6 singularity type (i.e., no monodromy in the IV^* fiber):

$$\mathcal{C}_{\text{tuned}} = \begin{array}{c} \mathfrak{e}_6 \quad \mathfrak{su}(3) \quad \mathfrak{e}_6 \\ 5 \quad 1 \quad 3 \quad 1 \quad 6 \quad 1 \end{array}. \quad (6.5)$$

This still satisfies the gauging condition, so no further blowups would be required in that case either.

Of course, there is no need to stop at a single additional blowup. Adding another blowup on the same configuration, we can instead take:

$$\mathcal{C}_{\text{nn-min}} = \begin{array}{|c|c|c|} \hline & 1 & \\ \hline 41 & 6 & 1 \\ \hline \end{array}. \quad (6.6)$$

Going through the blowups of the base in this case, we have:

$$\mathcal{C}_{\text{nn-min}} \rightarrow \begin{array}{|c|c|c|} \hline & 1 & \\ \hline 5131 & 7 & 1 \\ \hline \end{array} \rightarrow \begin{array}{|c|c|c|} \hline & 1 & \\ \hline 51321 & 8 & 1 \\ \hline \end{array} \quad (6.7)$$

There are clearly many possible ways of introducing additional non-minimal blowups. To

avoid clutter, we have suppressed the minimal gauge algebras for these examples.

Some (but not all!) endpoint configurations admit an infinite sequence of such blowups. Consider for example the endpoint $\mathcal{C}_{\text{end}} = 3$. Adding successive blowups to the rightmost curve in the graph, we reach, after k blowups, a configuration:

$$\mathcal{C}_{\text{n-min}} = \underbrace{42\dots 21}_k. \quad (6.8)$$

Now, this admits a consistent resolution to non-Higgsable clusters because the configuration $42\dots 2$ is an endpoint configuration with “room to spare” in the minimal resolution.

Many theories only admit a finite number of additional blowups. This appears to be the generic situation when there are a sufficiently large number of -2 curves in an endpoint. To give an example of this type, consider the endpoint given by the E_7 graph:

$$\mathcal{C}_{E_7} = \begin{array}{|c|c|c|c|c|c|} \hline & & 2 & & & \\ \hline 2 & 2 & 2 & 2 & 2 & 2 \\ \hline \end{array} . \quad (6.9)$$

Blowing up any point eventually requires us to blowup the -2 curve which only touches the trivalent vertex. So, consider first blowing up at this point. There is then a triggered sequence of blowups, leading eventually to:

$$\mathcal{C}_{E_7} \rightarrow \dots \rightarrow \begin{array}{|c|c|c|c|c|c|c|c|} \hline & & & 3 & & & & \\ \hline & & & 1 & & & & \\ \hline 2 & 3 & 1 & 5 & 1 & 3 & 2 & 2 \\ \hline \end{array} . \quad (6.10)$$

Anywhere else we attempt to blowup will eventually force more than seven blowups on the -5 curve. So this theory only admits one extra blowup. From the structure of the NHCs, we can also read off the gauge symmetry for this theory:

$$\begin{array}{|c|c|c|c|c|c|c|c|} \hline & & & \mathfrak{su}(3) & & & & \\ \hline & & & \oplus & & & & \\ \hline \mathfrak{su}(2) & \mathfrak{g}_2 & \oplus & \mathfrak{f}_4 & \oplus & \mathfrak{g}_2 & \mathfrak{sp}(1) & \\ \hline \end{array} \quad (6.11)$$

This can be viewed as a gauging of the $\mathfrak{e}_8^{\oplus 3}$ flavor symmetries for the three E-string theories associated with the -1 curves, according to the connectivity of the diagram. For example, the \mathfrak{f}_4 factor gauges the diagonal subalgebra of $\mathfrak{e}_8^{\oplus 3}$.

There are also minimal theories which are completely rigid. An example of this type is the endpoint $\mathcal{C}_{\text{end}} = (12)$, i.e., a single -12 curve. Any further blowups would make the self-intersection too high, and the Kodaira-Tate type of the elliptic fiber is already maximally

singular. Another example is the E_8 endpoint with graph:

$$\mathcal{C}_{E_8} = \begin{array}{|c|c|c|c|c|c|c|} \hline & & 2 & & & & \\ \hline 2 & 2 & 2 & 2 & 2 & 2 & 2 \\ \hline \end{array} . \quad (6.12)$$

If we attempt to blowup anywhere, it will eventually involve the -2 curve which only touches the trivalent vertex. However, the sequence of forced blowups leads us to:

$$\mathcal{C}_{E_8} \rightarrow \dots \rightarrow \begin{array}{|c|c|c|c|c|c|c|c|c|c|c|c|c|c|c|} \hline & & & & & 3 & & & & & & & & & & \\ \hline & & & & & 2 & & & & & & & & & & \\ \hline & & & & & 2 & & & & & & & & & & \\ \hline & & & & & 1 & & & & & & & & & & \\ \hline 2 & 3 & 2 & 2 & 1 & (12) & 1 & 2 & 2 & 3 & 1 & 5 & 1 & 3 & 2 & 2 \\ \hline \end{array} , \quad (6.13)$$

which still needs a further blowup on the left leg of the graph. This in turn pushes the -12 curve beyond the saturation limit, so no blowups can be tolerated for this theory. Finally, a more involved class of such rigid theories is:

$$\mathcal{C}_{7A_N7} = \underbrace{72\dots27}_N. \quad (6.14)$$

Performing the minimal resolution, the self-intersection of the -7 curves shifts to -12 , and the self-intersection of the -2 curves also shifts to -12 . Any further blowups would lead to an inconsistent model.

7 Duality Moves

So far, our approach to classification has involved a two stage process. First, we give a choice of minimal base and singular elliptic fibration, and then proceed to supplement this class of theories. Supplementing involves possibly further blowups in the base, as well as decoration of all curves by a consistent choice of gauge algebra. In this way, we have given a systematic way of generating all possible SCFTs which can be realized in F-theory. This should be viewed as a “bottom up” approach to the classification of 6D SCFTs.

Given such a list of SCFTs, it is natural to ask whether there are any redundancies, i.e. non-trivial dualities between given presentations. Though a complete answer is beyond the scope of this work, in this section we change tack, and ask from a “top down” perspective (including fiber information as well as information about the base) how to understand which distinct elliptically fibered Calabi-Yau threefolds will lead to dual descriptions of the same SCFT.

The basic idea will be to determine a geometric notion of an irrelevant deformation of a given SCFT. If we have two F-theory models which can be connected by such irrelevant de-

formations, they will flow to the same superconformal fixed point, and so will be deemed dual descriptions of the same theory. Our task therefore amounts to giving a precise geometric criterion for establishing physical equivalence.

First of all, we find that there are no dualities between the minimal 6D SCFTs. The reason is simply that such theories are fully specified by the generic choice of elliptic fibration with minimal singular behavior, so no irrelevant deformations of the geometry are available to connect these theories. However, once we start supplementing these cases to reach non-minimal theories, there are in principle various irrelevant deformations available which can connect different models.

The main duality move we discover involves the rearrangement of configurations of the form $1, 2, \dots, 2$, i.e. a string of undecorated curves with a -1 curve followed by some number of -2 curves. Generic blowups of the base involve attaching such chains to a point of a curve Σ in an endpoint configuration. Irrelevant deformations of the model correspond to moving such intersection points around, and possibly fragmenting such chains to smaller ones, or conversely, combining them to form a longer chain. For example, there is a duality operation of the form:¹⁴

$$\underbrace{2, \dots, 2, 1}_k, \Sigma, \underbrace{1, 2, \dots, 2}_l \longleftrightarrow \Sigma, \underbrace{1, 2, \dots, 2}_{k+l}. \quad (7.1)$$

This means that if we have two non-minimal blowups of a base, we can always move these chains around to take a representative presentation with a single chain of $1, 2, \dots, 2$.

The way we establish this duality move (as well as other duality operations) is somewhat technical, but we include it here for completeness. We begin with a base B corresponding to one of our endpoints, which takes the form \mathbb{C}^2/Γ . There is a one-dimensional representation V_m of Γ corresponding to $-mK_B$, and we can build appropriate spaces¹⁵ $(\mathbb{C}^2 \times V_m)/\Gamma$ in which x, y, f, g take values (for $m = 2, 3, 4, 6$, respectively), and define an elliptic fibration by the familiar Weierstrass equation $y^2 = x^3 + fx + g$. We include the case of trivial Γ in our considerations.

Because B is non-compact, there is no limit on the degrees of monomials in the \mathbb{C}^2 coordinates which can occur in f and g . However, for any specific SCFT, the degrees of monomials which can affect that SCFT are bounded. We will work with f and g polynomials of some fixed large degree, keeping in mind that we can enlarge the allowed degree if necessary.

For each pair (f, g) , there is either a specific blowup of B uniquely determined by the pair over which (f, g) produce a nonsingular F-theory model, or (f, g) are too singular to produce a nonsingular F-theory model on any blowup. We will now describe how to determine the blowup, and whether it exists.

We begin with the blowup $B_k \rightarrow B$ which is the minimal resolution of singularities of

¹⁴Note that the values of k and l are always bounded above, since we need to be able to blow down all -1 curves to reach a consistent endpoint configuration.

¹⁵These spaces do not always form bundles, but can be treated as coherent sheaves if the need arises.

the orbifold. We use k to label the number of compact curves on B_k . The Weierstrass coefficients f and g pull back to sections f_k, g_k of appropriate line bundles on B_k . There are three possibilities. First, if f_k vanishes to order at least 4 and g_k vanishes to order at least 6 on any (compact) curve on B_k , then we discard (f, g) as these coefficients cannot lead to a nonsingular F-theory model on any blowup of B_k .

Second, if at every point on B_k , either the multiplicity of f_k at the point is at most 3 or the multiplicity of g_k at the point is at most 5, then we do not need any further blowups: (f_k, g_k) define a nonsingular F-theory model over B_k itself.

Third, if neither of the first two cases hold, then there are finitely many points on B_k at which f_k has multiplicity at least 4 and g_k has multiplicity at least 6; pick one such point and blow it up, to obtain a new surface B_{k+1} and a blowdown map $\rho : B_{k+1} \rightarrow B_k$. We define $f_{k+1} = \rho^*(f_k)/\sigma^4$ and $g_{k+1} = \rho^*(g_k)/\sigma^6$, where $\sigma = 0$ is a defining equation for the -1 curve created by the blowup. Then (f_{k+1}, g_{k+1}) are sections of the appropriate bundles to be the Weierstrass coefficients of an F-theory model over B_{k+1} .

We now repeat this process for B_{k+1} , obtaining the same three alternatives as before. Since our polynomials have only a finite number of terms, and each of those multiplicity requirements imposes linear conditions on the terms in the polynomials, for any specific (f, g) this process must stop after a finite number of steps. At the end of the process, either the pair (f, g) has been eliminated due to excessive vanishing along some curve, or a blowup B_N (with N curves) has been obtained over which (f_N, g_N) define a nonsingular F-theory model. Note that no further blowups are allowed with this particular f and g .

In the blown up phase, the F-theory model defined by (f_N, g_N) has a number of characteristics: there are N tensor multiplets, gauge multiplets which are determined by the Kodaira-Tate singularity types along the various curves in the configuration, charged matter multiplets which are determined by the way the curves in the configuration meet the discriminant locus, and neutral matter multiplets which are determined by the polynomials f_N and g_N . When we shrink the configuration of curves on B_N to obtain a superconformal fixed point, most of the higher degree terms in f_N and g_N will not affect the actual fixed point we reach: They are associated with irrelevant deformations of the SCFT. The key point is that the leading order behavior of the singular fiber still controls the choice of SCFT we reach.

In particular, even though there is no Lagrangian description available, the singularity of the elliptic fiber remains well-defined, so there is still a notion of the ‘‘gauge algebra’’ associated with the singular model. We saw examples of this type in section 6 where we could decorate a minimal endpoint configuration by a higher order singularity type.

As explained in section 6, to each blown up nonsingular F-theory model, then, we can associate a graph describing the configuration of curves, and we can decorate each node of this graph with a gauge algebra consistent with a local gauging/gluing condition. To reach the superconformal fixed point, we then pass to the strongly coupled regime of this theory by shrinking the curves in the base to zero size. Note that since the elliptic model is governed

by a complex equation, it is still possible to track the behavior of the geometry in this limit.

In mathematical terms, the restriction on these new labels is that each curve must be labeled with a singularity which is at least as singular as the minimal singularity for that curve (i.e., the singularity in a maximally Higgsed model with the same curve configuration). Moreover, the singularities on two curves which meet cannot be so bad that they force a point of multiplicities $(4, 6)$ in f and g at their intersection. The singularity types are characterized by orders of vanishing of f_N and g_N as well as some data about whether certain expressions built from f_N and g_N have single-valued square roots (i.e., monodromy in the fiber). For further discussion see for example [51].

As an example, let us return to a case briefly discussed in section 6. Starting from the trivial endpoint $B_{\text{end}} = \mathbb{C}^2$, consider all of the ways to blow up three times, giving a connected configuration of curves. The first blowup produces a -1 curve, and the second blowup must be somewhere along it, yielding a 12 configuration. The third blowup can either be on the left curve (giving 122), at the intersection point (giving 213) or on the right curve (giving 131). Note that each of the latter two cases contain a -3 curve, and so have an $\mathfrak{su}(3)$ gauge symmetry at least.

We claim that the 213 configuration leads to the same SCFT as the 131 configuration. The mathematical details are given in Appendix E, so for now we focus on the broad features of the analysis. Consider the 131 model. We seek an irrelevant deformation which connects it to the 213 model. Now, the 131 model can be viewed as a -3 curve with two marked points, i.e., the locations where the -1 curves intersect our -3 curve. In the SCFT limit, we shrink all curves to zero size, including the -3 curve. As we shrink the -3 curve, the two -1 curves inevitably sit on top of one another. So, moving these two marked points around on the -3 curve corresponds to an irrelevant deformation. We choose to move the two marked points on top of each other. In this limit, the pair of -1 curves are on top of each other, and it is better to view this as the 213 model obtained from blowing up the intersection of the -1 curve and -2 curve in the configuration 12. Since the motion of points is a higher order contribution to the elliptic model, it is an irrelevant deformation, so we conclude that the configurations 213 and 131 specify the same SCFT; The different blowups simply label different chambers of the Coulomb branch. Indeed, in both the 213 and 131 model, we can regard the configuration as a -3 curve (which carries gauge symmetry) meeting some curves which carry no gauge symmetry. In fact, if we blow down the other two curves, we will find the points to be blown up labeled by the zeros of a polynomial on the remaining curve. When those zeros are distinct, we get two -1 's whereas when there is a double zero, we get the 12 chain by blowing up the same point twice in succession. Further, we see that upon blowing down one of the -1 curves in either 213 or 131, we reach a 12 theory with a decorated -2 curve. We can summarize this by the flows:

$$\begin{array}{ccccccc}
 & & \mathfrak{su}(3) & \xrightarrow{RG} & \mathfrak{su}(3) & \xrightarrow{RG} & \\
 2 & 1 & 3 & & 1 & 2 & 1 & 2
 \end{array} \tag{7.2}$$

Proceeding in this way, we can also see that the generic configuration 122 defines a different SCFT. To see this, observe that upon blowdown of a -1 curve in the configurations 213 and 131, we reach:

$$\mathcal{C}_{\text{tuned}} = \begin{array}{c} \mathfrak{su}(3) \\ 1 \quad 2 \end{array}, \quad (7.3)$$

i.e., a -2 curve decorated by a singular Kodaira-Tate fiber. This is to be contrasted with the blowdown of 122 to $\mathcal{C}_{\text{generic}} = 12$ with no singular elliptic fiber. The conclusion is that there is a further relevant deformation/unfolding from $\mathcal{C}_{\text{tuned}}$ to $\mathcal{C}_{\text{generic}}$. This is a relevant deformation, because it affects the leading order behavior of the singularity type.

We formulate this as the general principle summarized near line (7.1). For any curve Σ in a configuration carrying a gauge algebra, consider all of the -1 curves or $122 \dots 2$ chains meeting Σ . (A single -1 curve can be thought of as a chain with one link.) Then these chains of -1 and -2 curves can be rearranged into other chains of different lengths without changing the SCFT, as long as the total number of curves involved remains constant. This is the same thing which happens when considering multiple small instantons: if there are k of them overall, it does not matter how they are grouped into subsets, only the total instanton number k matters.

Finally, we are ready to state our notion of when two SCFTs are the same, i.e. they are connected by irrelevant deformations in the geometry. Let us fix an equivalence class of labeled graphs (i.e., allowing the rearrangements described in the previous paragraph) and consider the set of all (f, g) whose resolution produces this labeled graph. Since the conditions to have points of multiplicity $(4, 6)$ or to have vanishing of certain orders along certain curves are algebraic conditions on the coefficients appearing in f and g , the set of (f, g) producing a given class is a (locally closed) algebraic variety. Moreover, it is apparent that this variety is irreducible, because the choices being made when blowing up in order to obtain the correct graph are always of the form “choose a point to blow up which lies on a particular curve,” and that produces an irreducible variety. We find in this way the precise set of (f, g) which lead to a given SCFT.

This point of view is also very useful for determining flows between fixed points. There are two main types of flow to consider. First, if we reduce the singularity type of the fiber by a (partial) Higgs mechanism, we will flow between the resulting SCFTs. That is, if we retain the same graph but vary the labels, decreasing some of the gauge symmetries, we produce a flow among SCFTs. In the UV SCFT, Higgsing of this kind is carried out by allowing additional variations of (f, g) . The set of (f, g) with smaller singularities will contain in its closure the set of (f, g) with larger singularities, so moving into the larger set in the UV acts as a relevant deformation in the IR.

Second, we could blow down a -1 curve again giving a flow between fixed points. That flow is to be understood as follows:¹⁶ first blow down the -1 , and then deform (f_{N-1}, g_{N-1})

¹⁶Of course, this is just the extremal transition first described in [20].

to give a nonsingular F-theory model on B_{N-1} . That second step might not always be possible, or if possible, it might require changing the gauge algebra (in the resolved phase), but in the simplest of cases the gauge algebra will be the one inherited from that of B_N .

As a simple example, consider a configuration 413, with an $\mathfrak{so}(8)$ gauge algebra on the -4 curve and an $\mathfrak{su}(3)$ gauge algebra on the -3 curve. If we blow down the -1 curve, we still have the same order of vanishing of f and g along those curves (i.e., f vanishes to order 2 on both curves while g vanishes to order 3 on the -3 curve and to order 2 on the -2 curve. The (f, g) we started with will have a point of multiplicity $(4, 6)$ at the intersection, but that is not forced by the orders of vanishing, so there is a deformation which keeps the orders of vanishing (i.e., keeps those gauge algebras) while reducing the multiplicities of f and g at the intersection point to 4 and 5. We thus get a flow from the (maximally Higgsed) 413 configuration to a (non-maximally Higgsed) 32 configuration. Of course, we can then generate another flow by a Higgs mechanism which further reduces the gauge symmetries to \mathfrak{g}_2 and $\mathfrak{su}(2)$. We summarize this with the following diagram of RG flows:

$$\begin{array}{ccccccc} \mathfrak{so}(8) & & \mathfrak{su}(3) & \xrightarrow{RG} & \mathfrak{so}(8) & \mathfrak{su}(3) & \xrightarrow{RG} & \mathfrak{g}_2 & \mathfrak{su}(2) \\ 4 & 1 & 3 & & 3 & 2 & & 3 & 2 \end{array} . \quad (7.4)$$

8 Conclusions

In this paper we have studied geometrically realized superconformal field theories which can arise in compactifications of F-theory. Our primary claim is that minimal 6D SCFTs are captured by F-theory on the non-compact base \mathbb{C}^2/Γ with Γ a discrete subgroup of $U(2)$. Furthermore, one can obtain additional non-minimal SCFTs in two possible ways: first, by bringing in a number of additional E-string theories and second, by decorating a configuration of curves with a non-minimal gauge algebra. Both these operations lead to SCFTs with more degrees of freedom that can be deformed to flow down to lower theories, including all of the minimal ones. In the rest of this section we discuss some avenues of future investigation.

It is natural to ask whether there are additional SCFTs in six dimensions. Our list includes all the known examples of SCFTs in six dimensions that we are aware of, as well as a vast number of previously unknown examples. Based on this, it is tempting to conjecture that our method generates the full list of 6D SCFTs. It would be interesting to see if this is true.

We have fully classified the minimal 6D SCFTs and have indicated how to go about classifying non-minimal ones by introducing further blowups in the base, and decorating a graph of curves by a non-minimal gauge algebra. It would be quite instructive to give an explicit characterization of this class as well.

Regardless of whether there are even more 6D SCFTs outside our list, it should be clear that we have established the existence of a vast number of previously unknown $(1, 0)$ theories.

This should provide an excellent theoretical laboratory for gaining further insight into the workings of conformal theories in six dimensions.

For example, in this paper we have mainly focussed on the singular limit associated with a given conformal fixed point. To gain further insight into the structure of these theories, it would be exciting to fully map out the various branches of moduli space. We expect that this should be possible using the geometry of the F-theory model.

It would also be interesting to study compactifications of our $(1, 0)$ theories to lower dimensions and determine which ones flow to an interacting lower-dimensional SCFT. For the case of E -string theories this has already been studied and leads to interesting theories in lower dimensions. It is reasonable to believe that this may also be the generic story for many of the additional $(1, 0)$ SCFTs we have discovered in six dimensions.

Finally, we have discovered several new infinite families of $(1, 0)$ SCFTs which are labeled by an integer N which can be taken arbitrarily large. It would be interesting to determine whether there is a smooth large N limit of these theories, and a corresponding gravity dual, perhaps along the lines of [52].

Acknowledgements

We thank M. Del Zotto, B. Haghighat, T. Dumitrescu and E. Witten for helpful discussions. We also thank the 2013 Summer Workshop at the Simons Center for Geometry and Physics for hospitality, where some of this work was completed. The work of JJH and CV is supported by NSF grant PHY-1067976. The work of DRM is supported by NSF grant PHY-1307513.

A Instructions for Using the Mathematica Notebook

In the arXiv submission we also include a sample Mathematica notebook called `BlowUpDown.nb`. This file computes the minimal resolution of a candidate endpoint configuration, and also determines whether a given linear chain of NHCs blows down to a consistent endpoint.

To access the Mathematica notebook, proceed to the URL where the arXiv submission and abstract is displayed. On the righthand side of the webpage, there will be a box labeled “Download:”. Click on the link “Other formats”, and then under the boldfaced line “Source” click on the link “[Download source]”. A download of a zipped file should then commence. In some cases, it may be necessary to append the ending `.tar.gz` to the end of the file. The set of submission files along with the Mathematica notebook can then be accessed by unzipping this file. For further instruction on unzipping such files, see for example <http://arxiv.org/help/unpack>.

The two main functions in the file are `BlowUP` and `BlowDOWN` which take as input a vector of integers $\{a_1, \dots, a_r\}$. The respective outputs are a computation of the minimal resolution, and sequential blowdown of all -1 curves. The functions also indicate if a configuration of curves contains various inconsistencies. We also include an example of how to perform a sweep over all configurations for ten or fewer curves in an A-type graph. We have not optimized the notebook scripts for efficiency, but even so, on a (circa 2013) laptop the full computation only takes about half a day to finish.

B Constraints on Contractible Curve Configurations

Suppose that $\Sigma_1, \dots, \Sigma_r$ are compact complex curves on a complex surface B . Mumford [31] showed that if those curves can contract to a point (smooth or singular), then the negative of the intersection matrix

$$A_{ij} = -(\Sigma_i \cdot \Sigma_j) \tag{B.1}$$

is positive definite. Conversely, if that matrix is positive definite, then Grauert [33] showed that the collection of curves can be contracted to a complex analytic (singular) point. Artin [32] showed that if, in addition, the singularity satisfies a condition known as “rationality” [53], the contraction is guaranteed to be an algebraic singular point. In fact, all orbifolds are rational singularities, so when we contract we stay within the realm of algebraic varieties.

Given any divisor D on B , there are nonnegative rational numbers a_i such that

$$\left(D - \sum a_i \Sigma_i\right) \cdot \Sigma_j \geq 0 \text{ for all } j, \tag{B.2}$$

and

$$\left(D - \sum a_i \Sigma_i\right) \cdot \Sigma_j = 0 \text{ whenever } a_j \neq 0. \tag{B.3}$$

The \mathbb{Q} -divisor $N = \sum a_i \Sigma_i$ is called the *negative part of the Zariski decomposition of D* [54].

The coefficients a_i depend on the divisor D .

Let $\sum \alpha_i \Sigma_i$ be the negative part of the Zariski decomposition of $-K_B$. Then any section of $-mK_B$ must vanish to order at least $m\alpha_i$ along C_i . Since $m\alpha_i$ is in general a rational number, what this means in practice is that the order of vanishing must be the next highest integer (as a minimum).

From this we infer an important property: if $\alpha_i > 5/6$, then f and g vanish along Σ_i to orders 4 and 6, respectively. In particular, a base containing such a configuration cannot support a nonsingular F-theory model, even after blowing up the base further. To see this, notice that $4\alpha_i > 10/3$ so the minimum order of vanishing of f is 4, and $6\alpha_i > 5$ so the minimum order of vanishing of g is 6.

Now we use this property to formulate some constraints on contractible curve configurations. First, every curve Σ in the configuration must have arithmetic genus $g = 0$. For if Σ were a curve with positive arithmetic genus, then $K_B \cdot \Sigma + \Sigma \cdot \Sigma = 2g - 2 \geq 0$. It follows that

$$1 + \frac{2-2g}{\Sigma \cdot \Sigma} \geq 1 > \frac{5}{6} \text{ and } \left(-K_B - \left(1 + \frac{2-2g}{\Sigma \cdot \Sigma} \right) \Sigma \right) \cdot \Sigma = 0. \quad (\text{B.4})$$

Thus, the coefficient of Σ in the negative part of the Zariski decomposition of $-K_B$ is greater than $5/6$, so there is no nonsingular F-theory model supported by this surface.

Second, given two curves Σ and Σ' , they can meet in at most one point. For if $\Sigma \cdot \Sigma' \geq 2$, then

$$(-K_B - \Sigma - \Sigma') \cdot \Sigma = 2 - \Sigma' \cdot \Sigma \leq 0, \quad (\text{B.5})$$

and similarly $(-K_B - \Sigma - \Sigma') \cdot \Sigma' \leq 0$. Let $a\Sigma + a'\Sigma'$ be the negative part of the Zariski decomposition of $-K_B - \Sigma - \Sigma'$. Then $(1+a)\Sigma + (1+a')\Sigma'$ is the negative part of the Zariski decomposition of $-K_B$. Since $1+a$ and $1+a'$ are both greater than $5/6$, f and g vanish to too high an order along Σ and Σ' so there is no nonsingular F-theory model.

Finally, let $\Sigma_1, \dots, \Sigma_r$ be a loop (of curves of genus 0). Then

$$\left(-K_B - \sum_i \Sigma_i \right) \cdot \Sigma_j = -K_B \cdot \Sigma_j - \Sigma_j \cdot \Sigma_j - \left(\sum_{i \neq j} \Sigma_i \right) \cdot \Sigma_j = 2 - 2 = 0, \quad (\text{B.6})$$

since each curve in the loop meets exactly two other curves in the loop. Again, this shows that the coefficients in the negative part of the Zariski decomposition of $-K_B$ are all 1, and in particular all greater than $5/6$, so there is no nonsingular F-theory model.

As a special case, notice that three curves passing through a common point have the same intersection properties as three curves in a loop, so this is excluded as well.

The conclusion is that, in order to support a nonsingular F-theory model (even after blowing the base up further), our collection of curves must all be rational, meeting two at a time in distinct points and with no tangencies (i.e., it has “normal crossings”), and the dual graph of the collection must form a tree.

C The Gluing Condition in the Maximally Higgsed Case

Let B be a neighborhood of a contractible configuration of compact curves which supports a nonsingular F-theory model, and let E be a -1 curve on B . We choose a nonsingular F-theory model which is maximally Higgsed, and consider the other curves Σ_j in the configuration which meet E . The “gluing condition” which we would like to verify states that the direct sum of the Lie algebras \mathfrak{g}_{Σ_j} must be a subalgebra of \mathfrak{e}_8 .

Verifying this condition means analyzing all of the ways in which the other curves can meet E . In fact, table 3 of [21] already listed all ways that -1 curves can meet non-Higgsable clusters, but here we are much more constrained: because our -1 curves are part of a contractible configuration of curves, and the configuration must have normal crossings even after blowing down the -1 curve, each (-1) curve can meet at most two other curves (and it will meet them with intersection number 1).

Since each of the gauge algebras which occurs in a non-Higgsable cluster is a subalgebra of \mathfrak{e}_8 , the condition is automatically satisfied if E meets 0 or 1 curves. In the case of 2 curves, blowing down E gives us two components of the discriminant locus which meet each other (or “collide”): this situation was analyzed and applied to F-theory long ago [50, 8]. However, those works had an additional hypothesis (“well-defined J invariant”) which is not relevant here, so we need to do the analysis again.

Before beginning, we recall a refinement of the classification of clusters from [21]. Each curve in each cluster not only carries a gauge algebra, but a specific Kodaira-Tate type, labeled by the orders of vanishing of f and g along the curve. This even applies to the curve in the 3, 2, 2 cluster which carries no gauge algebra: it has a Kodaira type labeled by a single order of vanishing of both f and g ; we will label this in parallel to the other gauge algebras as \mathfrak{h}_0 (following the notation of [55].)¹⁷ The gauge algebra $\mathfrak{su}(2)$ actually has two realizations from this point of view; we refer to one of them as $\mathfrak{sp}(1)$ in order to keep them straight.

Here is a list of all possible gauge algebras, together with their Kodaira conditions (where \mathfrak{h}_0 is trivial as an algebra).

algebra	\mathfrak{h}_0	$\mathfrak{su}(2)$	$\mathfrak{sp}(1)$	$\mathfrak{su}(3)$	\mathfrak{g}_2	$\mathfrak{so}(7)$	$\mathfrak{so}(8)$	\mathfrak{f}_4	\mathfrak{e}_6	\mathfrak{e}_7	\mathfrak{e}_8
$\text{ord}_{\Sigma}(f)$	1	1	2	2	2	2	2	3	3	3	4
$\text{ord}_{\Sigma}(g)$	1	2	2	2	3	3	3	4	4	5	5

(C.1)

The 3, 2 cluster has algebras $\mathfrak{g}_2, \mathfrak{su}(2)$, the 3, 2, 2 cluster has algebras $\mathfrak{g}_2, \mathfrak{sp}(1), \mathfrak{h}_0$, and the 2, 3, 2 cluster has algebras $\mathfrak{su}(2), \mathfrak{so}(7), \mathfrak{su}(2)$.

Our next observation is that a curve with algebra $\mathfrak{sp}(1)$ cannot be one of two curves meeting E . This is because the only curve carrying $\mathfrak{sp}(1)$ is the central curve in a 3, 2, 2

¹⁷In fact, as pointed out in [55], when compactified to four dimensions, this Kodaira type leads to the Argyres-Douglas SCFT [56].

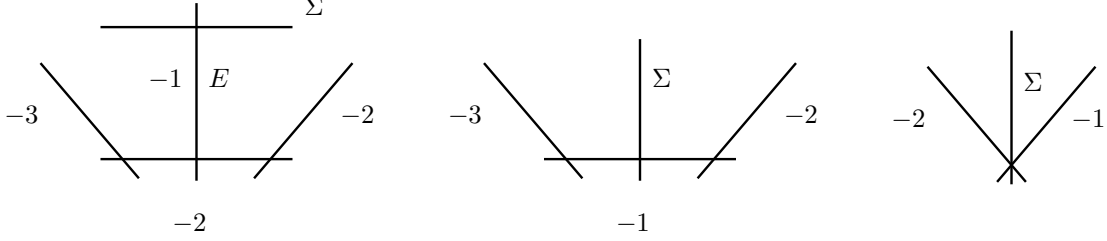


Figure 2: Blowing down a configuration containing $\mathfrak{sp}(1)$

cluster. If it was one of two curves meeting E , then as shown in figure 2, after two blowdowns we lose normal crossings, which is not permitted. Thus, whenever we see orders of vanishing $(2, 2)$ for (f, g) , we may assume that the gauge algebra is $\mathfrak{su}(3)$.

Now our basic computation is to consider a chain of three curves Σ_L, E, Σ_R and specify the orders of vanishing of f and g along them as $(a_L, b_L), (a, b)$, and (a_R, b_R) . If we contract E we will find a point where the multiplicities of f and g are at least $a_L + a_R$ and $b_L + b_R$, respectively. Therefore, $a \geq a_L + a_R - 4$ and $b \geq b_L + b_R - 6$. Let a_{\min} be the larger of $a_L + a_R - 4$ and 0, and similarly let b_{\min} be the larger of $b_L + b_R - 6$ and 0.

Now, if $a_{\min} \geq 1$ and $b_{\min} \geq 2$ there will be a gauge algebra associated to E , contrary to our assumption that we are working with a maximally Higgsed F-theory model. Thus, there are upper bounds on a_{\min} and b_{\min} and it is straightforward to make a table of allowed possibilities.

We give the table in two parts: first, there are some cases which do not actually occur:

\mathfrak{g}_{Σ_L}	(a_L, b_L)	(a_{\min}, b_{\min})	(a_R, b_R)	\mathfrak{g}_{Σ_R}
$\mathfrak{su}(2)$	(1, 2)	(1, 1)	(4, 5)	\mathfrak{e}_8
$\mathfrak{su}(3)$	(2, 2)	(1, 1)	(3, 5)	\mathfrak{e}_7
$\mathfrak{so}(7)$ or $\mathfrak{so}(8)$	(2, 3)	(1, 1)	(3, 4)	\mathfrak{f}_4 or \mathfrak{e}_6
\mathfrak{g}_2 or $\mathfrak{so}(7)$ or $\mathfrak{so}(8)$	(2, 3)	(1, 1)	(3, 4)	\mathfrak{e}_6

(C.2)

The first two cases do not occur because the point of intersection of E and Σ_R has multiplicities at least $(4, 6)$ and thus it must be blown up (contrary to our assumption that B is the base of a nonsingular F-theory model). The last two cases do not occur because of an interesting subtlety. Although E carries no gauge symmetry, it is of Kodaira type \mathfrak{h}_0 in those cases, and in particular $\{f = 0\}$ must meet Σ_L and $\{g = 0\}$ must meet Σ_R .

On the other hand, if Σ_R has gauge algebra \mathfrak{e}_6 then $(-6K_B - 4\Sigma_R) \cdot \Sigma_R = -24 + 24 = 0$ so Σ_R cannot meet $\{g = 0\}$. If Σ_L has gauge algebra $\mathfrak{so}(8)$ then $(-4K_B - 2\Sigma_L) \cdot \Sigma_L = -8 + 8 = 0$ so Σ_L cannot meet $\{f = 0\}$. And finally, if Σ_L has gauge algebra $\mathfrak{so}(7)$ then Σ_L is the central curve is a 2, 3, 2 cluster, and for such a cluster, the effective divisor from the Zariski decomposition is $-4K_B - \Sigma'_L - 2\Sigma_L - \Sigma''_L$, which has intersection number 0 with Σ_L . This again implies that Σ_L cannot meet $\{f = 0\}$.

Having excluded those four cases, we are left with the two kinds of cases. First, there are those in which both $a_L + a_R - 4$ and $b_L + b_R - 6$ are nonnegative:

\mathfrak{g}_{Σ_L}	(a_L, b_L)	(a_{\min}, b_{\min})	(a_R, b_R)	\mathfrak{g}_{Σ_R}
\mathfrak{h}_0	(1, 1)	(0, 0)	(3, 5)	\mathfrak{e}_7
\mathfrak{h}_0	(1, 1)	(1, 0)	(4, 5)	\mathfrak{e}_8
$\mathfrak{su}(2)$	(1, 2)	(0, 0)	(3, 4)	\mathfrak{f}_4 or \mathfrak{e}_6
$\mathfrak{su}(2)$	(1, 2)	(0, 1)	(3, 5)	\mathfrak{e}_7
$\mathfrak{su}(3)$	(2, 2)	(1, 0)	(3, 4)	\mathfrak{f}_4 or \mathfrak{e}_6
\mathfrak{g}_2 or $\mathfrak{so}(7)$ or $\mathfrak{so}(8)$	(2, 3)	(0, 0)	(2, 3)	\mathfrak{g}_2 or $\mathfrak{so}(7)$ or $\mathfrak{so}(8)$
\mathfrak{g}_2	(2, 3)	(1, 1)	(3, 4)	\mathfrak{f}_4

(C.3)

Second, we have cases where either $a_L + a_R - 4$ or $b_L + b_R - 6$ is negative; this means that at least one additional zero of f or g occurs at the intersection point, in addition to the ones coming from Σ_L and Σ_R . These cases are:

\mathfrak{g}_{Σ_L}	(a_L, b_L)	(a_{\min}, b_{\min})	(a_R, b_R)	\mathfrak{g}_{Σ_R}
\mathfrak{h}_0	(1, 1)	(0, 0)	(1, 1)	\mathfrak{h}_0
\mathfrak{h}_0	(1, 1)	(1, 0)	(1, 2)	$\mathfrak{su}(2)$
\mathfrak{h}_0	(1, 1)	(0, 0)	(2, 2)	$\mathfrak{su}(3)$
\mathfrak{h}_0	(1, 1)	(0, 1)	(2, 3)	\mathfrak{g}_2 or $\mathfrak{so}(7)$ or $\mathfrak{so}(8)$
\mathfrak{h}_0	(1, 1)	(1, 0)	(3, 4)	\mathfrak{f}_4 or \mathfrak{e}_6
$\mathfrak{su}(2)$	(1, 2)	(0, 0)	(1, 2)	$\mathfrak{su}(2)$
$\mathfrak{su}(2)$	(1, 2)	(1, 0)	(2, 2)	$\mathfrak{su}(3)$
$\mathfrak{su}(2)$	(1, 2)	(0, 0)	(2, 3)	\mathfrak{g}_2 or $\mathfrak{so}(7)$ or $\mathfrak{so}(8)$
$\mathfrak{su}(3)$	(2, 2)	(0, 1)	(2, 2)	$\mathfrak{su}(3)$
$\mathfrak{su}(3)$	(2, 2)	(1, 0)	(2, 3)	\mathfrak{g}_2 or $\mathfrak{so}(7)$ or $\mathfrak{so}(8)$

(C.4)

As can be easily seen, in each case listed in (C.3) and (C.4), we have $\mathfrak{g}_{\Sigma_L} \oplus \mathfrak{g}_{\Sigma_R} \subset \mathfrak{e}_8$.

D Resolution of Orbifold Singularities

As stated in the text, any chain of rational curves with self-intersections $-x_1, \dots, -x_r$ ($x_j \geq 2$) is the resolution of \mathbb{C}^2/Γ , where $\Gamma = A(x_1, \dots, x_r)$ is the cyclic group of order p generated by $(z_1, z_2) \mapsto (e^{2\pi i/p} z_1, e^{2\pi i q/p} z_2)$ and the continued fraction expansion of p/q has coefficients x_1, \dots, x_r . This goes back to work of Jung [35] and Hirzebruch [36], with the resolution described in modern language in [37].

We illustrate with the example $p/q = 24/7 = 4 - 1/(2 - 1/4)$, whose resolution we describe in terms of toric geometry, as illustrated in figure 3. The toric data begins with vectors $v_0 = (0, p)$ and $v_1 = (q, 1)$, and then continues with $v_{j-1} + v_{j+1} = x_j v_j$ where x_j are the continued fraction coefficients, ending with $v_{r+1} = (p, 0)$. (In our example, this produces

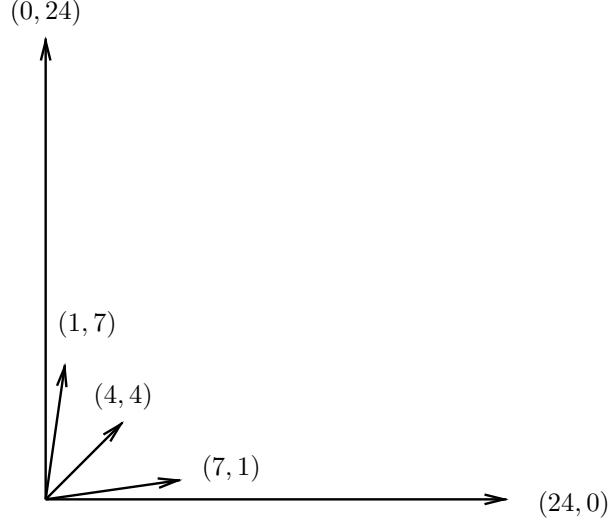


Figure 3: Toric data for the $(4, 2, 4)$ model, with $p/q = 24/7$.

the five vectors shown in the figure.) Each pair of adjacent vectors determines a coordinate chart in which the Laurent monomial $z_1^m z_2^n$ extends to a holomorphic function exactly if $(m, n) \cdot v_{j-1} \geq 0$ and $(m, n) \cdot v_j \leq 0$. In our example, we get four coordinate charts in this way, described as follows:

$$\begin{aligned}
 (\alpha_1, \beta_1) &= (z_1^{24}, z_1^{-7} z_2) \\
 (\alpha_2, \beta_2) &= (z_1^7 z_2^{-1}, z_1^{-4} z_2^4) = (\beta_1^{-1}, \alpha_1 \beta_1^4) \\
 (\alpha_3, \beta_3) &= (z_1^4 z_2^{-4}, z_1^{-1} z_2^7) = (\beta_2^{-1}, \alpha_2 \beta_2^2) \\
 (\alpha_4, \beta_4) &= (z_1 z_2^{-7}, z_2^{24}) = (\beta_3^{-1}, \alpha_3 \beta_3^4)
 \end{aligned} \tag{D.1}$$

In general, there will be $r + 1$ such coordinate charts (α_i, β_i) . The i^{th} exceptional divisor appears in both the i^{th} and the $(i + 1)^{\text{st}}$ charts.

If the string $x_1 \cdots x_r$ has an odd number $r = 2\ell + 1$ of entries, reads the same forwards and backwards (i.e., $x_{r+1-j} = x_j$, and has an even value $x_{\ell+1} = 2y - 2$ in the middle (all of which are satisfied in our example) then we can extend our cyclic group action by $(z_1, z_2) \mapsto (z_2, -z_1)$ in order to generate the group $D(y|x_1, \dots, x_\ell)$. This new element acts on the various coordinate charts in the resolution by

$$(\alpha_i, \beta_i) \mapsto (\pm \beta_{r+1-i}, \pm \alpha_{r+1-i}), \tag{D.2}$$

where the signs are determined by the degrees of the monomials occurring in the expressions for the coordinates.

The effect of this element is to exchange the ends of the chain, but the middle curve in

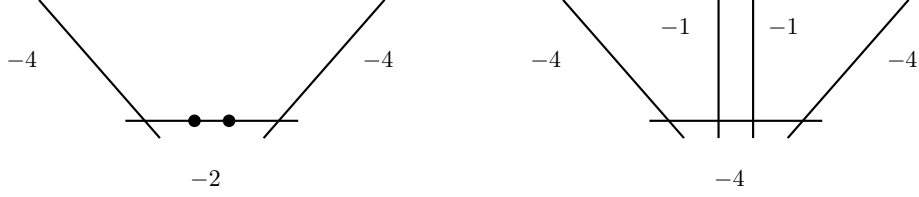


Figure 4: Blowing up the fixed points.

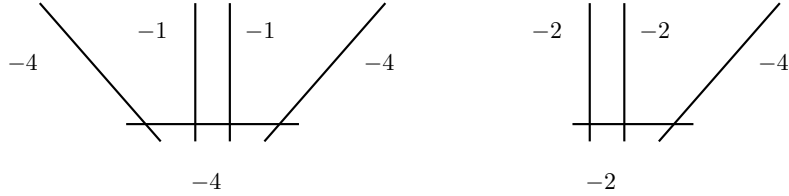


Figure 5: Taking the quotient.

the chain will be preserved. In our example, we see this as

$$(\alpha_2, \beta_2) \mapsto (-\beta_3, \alpha_3) = (-\alpha_2\beta_2^2, \beta_2^{-1}). \quad (\text{D.3})$$

We look for fixed points of this group action: at a fixed point, we have $\beta_2 = \beta_2^{-1}$, so $\beta_2 = \pm 1$. But then $\alpha_2(1 + \beta_2^2) = 0$ so $\alpha_2 = 0$. There are thus two fixed points on the middle curve, away from its intersections with the outer curves. These fixed points are indicated with a solid circle in the left half of figure 4.

To take the quotient by this additional group element, it is convenient to first blow up the fixed points of the group action, yielding the configuration depicted in the right half of figure 4. The group element acts as an involution on this configuration, fixing each of the -1 curves, acting nontrivially on the -4 curve at the bottom of the figure, and exchanging the other two -4 curves. (In more complicated examples, those “other” -4 curves will each be replaced by a long chain of curves, and those chains are exchanged.)

The result of this quotient operation is illustrated in figure 5, with the configuration before the quotient on the left, and the configuration after the quotient on the right. Note that the “bottom” curve was not a fixed curve and had its self-intersection divided by 2, whereas the fixed curves had their self-intersections double (from -1 to -2). The quotiented configuration is of type D_224 .

E Relevant and Irrelevant Deformations

In this Appendix, we give more details about an example considered in the text of blowing up a nonsingular point three times, from the point of view of the Weierstrass equation of

the F-theory model. The Weierstrass equation takes the form $y^2 = x^3 + fx + g$ where f and g are functions of coordinates z_1, z_2 on \mathbb{C}^2 . Our analysis is similar to that in [57].

The generic such Weierstrass equation does not lead to a blowup, nor is there any interesting conformal theory associated with it. To see a conformal theory (corresponding to blowing up the origin), we need f to have multiplicity at least 4 at the origin, and g to have multiplicity at least 6. That is,

$$\begin{aligned} f &= \sum_{k=4}^{\infty} \sum_{j=0}^k \varphi_{jk} z_1^{k-j} z_2^j \\ g &= \sum_{k=6}^{\infty} \sum_{j=0}^k \gamma_{jk} z_1^{k-j} z_2^j. \end{aligned} \tag{E.1}$$

One coordinate chart on the blowup is obtained by substituting $z_2 = z_1 \tilde{z}_2$, and defining

$$\begin{aligned} f_1 &= f/\tilde{z}_2^4 = \sum_{k=4}^{\infty} \sum_{j=0}^k \varphi_{jk} z_1^{k-4} \tilde{z}_2^j \\ g_1 &= g/\tilde{z}_2^6 = \sum_{k=6}^{\infty} \sum_{j=0}^k \varphi_{jk} z_1^{k-6} \tilde{z}_2^j. \end{aligned} \tag{E.2}$$

E.1 Multiplicities 6 and 8

We will explore various conditions one can put on the generic pair (f, g) given in (E.1) which will lead to different SCFTs. One condition we can impose is to ask that f has multiplicity at least 6 and g has multiplicity at least 8. That is, we assume that $\varphi_{jk} = 0$ whenever $k = 4, 5$ and $\gamma_{jk} = 0$ whenever $k = 6, 7$. In that case, after the blowup, f and g each vanish to order 2 along the exceptional divisor, which is reflected in the fact that z_1^2 divides each equation:

$$\begin{aligned} f_1 &= z_1^2 \sum_{k=6}^{\infty} \sum_{j=0}^k \varphi_{jk} z_1^{k-6} \tilde{z}_2^j \\ g_1 &= z_1^2 \sum_{k=8}^{\infty} \sum_{j=0}^k \varphi_{jk} z_1^{k-6} \tilde{z}_2^j. \end{aligned} \tag{E.3}$$

According to Kodaira's classification, the exceptional curve now has a gauge symmetry of $\mathfrak{su}(3)$ (i.e., type IV in Kodaira's notation).

To search for additional blowups, we consider f_1/z_1^2 and g_1/z_1^2 , looking for points of multiplicity 2 and 4 along the exceptional divisor. The easy way to test for this is to restrict

to the exceptional divisor (by setting $z_1 = 0$) and then look for multiple roots.

$$\begin{aligned} (f_1/z_1^2)|_{z_1=0} &= \sum_{j=0}^6 \varphi_{j,6} \tilde{z}_2^j \\ (g_1/z_1^2)|_{z_1=0} &= \sum_{j=0}^8 \varphi_{j,8} \tilde{z}_2^j. \end{aligned} \tag{E.4}$$

(The reason the sums have collapsed is that we needed to set the exponent of z_1 equal to zero, and doing so fixed the value of k .)

We now see that up to three points of multiplicity two are possible for $(f_1/z_1^2)|_{z_1=0}$, while only two points of multiplicity four are possible for $(g_1/z_1^2)|_{z_1=0}$. Of course, we want both of these multiplicities to happen, and at the same point.

If we wish to do one additional blowup, we need a common point of high multiplicity of both of these expressions, which we take to be at $\tilde{z}_2 = \lambda$. The condition for this is:

$$\begin{aligned} (\tilde{z}_2 - \lambda)^2 &| \sum_{j=0}^6 \varphi_{j,6} \tilde{z}_2^j \\ (\tilde{z}_2 - \lambda)^4 &| \sum_{j=0}^8 \varphi_{j,8} \tilde{z}_2^j. \end{aligned} \tag{E.5}$$

On the other hand, if we wish to do two additional blowups, then $(g_1/z_1^2)|_{z_1=0}$ must have two zeros of multiplicity 4, so it must have the form

$$\sum_{j=0}^8 \varphi_{j,8} \tilde{z}_2^j = (a\tilde{z}_2^2 + b\tilde{z}_2 + c)^4, \tag{E.6}$$

and we must also have $(a\tilde{z}_2^2 + b\tilde{z}_2 + c)^2$ as a divisor of $(f_1/z_1^2)|_{z_1=0}$.

All choices of quadratic polynomial lead to the same SCFT, and we see that when the quadratic polynomial has two distinct roots, we blow up in two distinct points yielding a configuration 131 whereas when there is a double root, we blow up the same point twice yielding a configuration 213.

E.2 Two Blowups Specified

Another condition we can put on the generic pair (f, g) given in (E.1) is to assume that two blowups can be done, and to choose coordinates so that the second blowup is at the origin of the (z_1, \tilde{z}_2) coordinate chart. That is, in equation (E.2), we wish to impose multiplicity 4 at the origin on f_1 and multiplicity 6 at the origin on g_1 .

We can do this by further restricting our original polynomials (E.1) as follows:

$$\begin{aligned}
f &= \sum_{\ell=8}^{\infty} \sum_{j=0}^{[\ell/2]} \varphi_{j,\ell-j} z_1^{\ell-2j} z_2^j \\
g &= \sum_{\ell=12}^{\infty} \sum_{j=0}^{[\ell/2]} \gamma_{j,\ell-j} z_1^{\ell-2j} z_2^j.
\end{aligned} \tag{E.7}$$

In other words, we have set the coefficients φ_{jk} to zero for $4 \leq k < 8 - j$, and the coefficients γ_{jk} to zero for $6 \leq k < 12 - j$.

The first blowup is again obtained by the coordinate change $z_2 = z_1 \tilde{z}_2$, giving

$$\begin{aligned}
f_1 &= \sum_{\ell=8}^{\infty} \sum_{j=0}^{[\ell/2]} \varphi_{j,\ell-j} z_1^{\ell-j-4} \tilde{z}_2^j \\
g_1 &= \sum_{\ell=12}^{\infty} \sum_{j=0}^{[\ell/2]} \gamma_{j,\ell-j} z_1^{\ell-j-6} \tilde{z}_2^j.
\end{aligned} \tag{E.8}$$

One of the coordinate charts in the second blowup is then obtained by the substitution $z_1 = \tilde{z}_1 \tilde{z}_2$, giving

$$\begin{aligned}
f_2 &= \sum_{\ell=8}^{\infty} \sum_{j=0}^{[\ell/2]} \varphi_{j,\ell-j} \tilde{z}_1^{\ell-j-4} \tilde{z}_2^{\ell-8} \\
g_2 &= \sum_{\ell=12}^{\infty} \sum_{j=0}^{[\ell/2]} \gamma_{j,\ell-j} \tilde{z}_1^{\ell-j-6} \tilde{z}_2^{\ell-12}.
\end{aligned} \tag{E.9}$$

In this coordinate chart, the first exceptional divisor is given by $\tilde{z}_1 = 0$, while the second exceptional divisor is given by $\tilde{z}_2 = 0$. If we wish to blow up a point on the first exceptional divisor, we look for points at which f and g have high multiplicity along the curve $\{\tilde{z}_1 = 0\}$. We write (E.9) as a series in \tilde{z}_1 :

$$\begin{aligned}
f_2 &= \varphi_{4,4} \tilde{z}_2^0 + (\varphi_{3,5} \tilde{z}_2^0 + \varphi_{4,5} \tilde{z}_2^1 + \varphi_{5,5} \tilde{z}_2^2) \tilde{z}_1 + O(\tilde{z}_1^2) \\
g_2 &= \gamma_{6,6} \tilde{z}_2^0 + (\gamma_{5,7} \tilde{z}_2^0 + \gamma_{6,7} \tilde{z}_2^1 + \gamma_{7,7} \tilde{z}_2^2) \tilde{z}_1 + O(\tilde{z}_1^2).
\end{aligned} \tag{E.10}$$

If we restrict f_2 and g_2 to $\tilde{z}_1 = 0$, we get constant polynomials, so they cannot have any zeros unless they vanish identically. If we set $\varphi_{4,4} = \gamma_{6,6} = 0$ so that zeros are possible, then $(f_2/\tilde{z}_1)|_{\tilde{z}_1=0}$ and $(g_2/\tilde{z}_1)|_{\tilde{z}_1=0}$ should have points of multiplicity 3 and 5, respectively, but this is not possible since each of those expressions is a quadratic polynomial in \tilde{z}_2 . Thus, those quadratic polynomials must also vanish identically, and we see that f and g each vanish twice along the first exceptional divisor. This puts us back in the case considered in the previous subsection.

On the other hand, if we wish to blow up a point on the second (most recently created) exceptional divisor, we can look for points to blow up by restricting equation (E.9) to $\tilde{z}_2 = 0$, giving

$$\begin{aligned} (f_2)_{\tilde{z}_2=0} &= \sum_{j=0}^4 \varphi_{j,8-j} \tilde{z}_1^{4-j} \\ (g_2)_{\tilde{z}_2=0} &= \sum_{j=0}^6 \gamma_{j,12-j} \tilde{z}_1^{6-j}. \end{aligned} \tag{E.11}$$

So the condition for a third blowup is the existence of a linear function $a\tilde{z}_1 + b$ such that

$$\begin{aligned} \sum_{j=0}^4 \varphi_{j,8-j} \tilde{z}_1^{4-j} &= (a\tilde{z}_1 + b)^4 \\ \sum_{j=0}^6 \gamma_{j,12-j} \tilde{z}_1^{6-j} &= (a\tilde{z}_1 + b)^6. \end{aligned} \tag{E.12}$$

This gives a configuration of type 122.

Notice that if $b = 0$, then the point we are blowing up is also on the first exceptional divisor. So in that case, f and g again vanish to order 2 along $\tilde{z}_1 = 0$ and we have enhanced gauge symmetry (and a different SCFT).

References

- [1] E. Witten, “Some comments on string dynamics,” [arXiv:hep-th/9507121](#).
- [2] A. Strominger, “Open P-Branes,” *Phys. Lett.* **B383** (1996) 44–47, [arXiv:hep-th/9512059](#).
- [3] E. Witten, “Small Instantons in String Theory,” *Nucl. Phys.* **B460** (1996) 541–559, [arXiv:hep-th/9511030](#).
- [4] O. J. Ganor and A. Hanany, “Small E_8 instantons and Tensionless Non Critical Strings,” *Nucl. Phys.* **B474** (1996) 122–140, [arXiv:hep-th/9602120](#).
- [5] N. Seiberg and E. Witten, “Comments on String Dynamics in Six Dimensions,” *Nucl. Phys.* **B471** (1996) 121–134, [arXiv:hep-th/9603003](#).
- [6] J. A. Minahan and D. Nemeschansky, “An $\mathcal{N} = 2$ superconformal fixed point with E_6 global symmetry,” *Nucl. Phys.* **B482** (1996) 142–152, [arXiv:hep-th/9608047](#).
- [7] J. A. Minahan and D. Nemeschansky, “Superconformal fixed points with E_n global symmetry,” *Nucl. Phys.* **B489** (1997) 24–46, [arXiv:hep-th/9610076](#).
- [8] M. Bershadsky and A. Johansen, “Colliding singularities in F-theory and phase transitions,” *Nucl. Phys.* **B489** (1997) 122–138, [arXiv:hep-th/9610111](#).
- [9] J. D. Blum and K. A. Intriligator, “New Phases of String Theory and 6d RG Fixed Points via Branes at Orbifold Singularities,” *Nucl. Phys.* **B506** (1997) 199–222, [arXiv:hep-th/9705044](#).
- [10] E. Witten, “Physical interpretation of certain strong coupling singularities,” *Mod. Phys. Lett. A* **11** (1996) 2649–2654, [arXiv:hep-th/9609159](#).
- [11] N. Seiberg, “Non-trivial fixed points of the renormalization group in six dimensions,” *Phys. Lett. B* **390** (1997) 169–171, [arXiv:hep-th/9609161](#).
- [12] P. S. Aspinwall, “Point-like instantons and the $\text{Spin}(32)/\mathbb{Z}_2$ heterotic string,” *Nucl. Phys. B* **496** (1997) 149–176, [arXiv:hep-th/9612108](#).
- [13] K. A. Intriligator, “RG fixed points in six dimensions via branes at orbifold singularities,” *Nucl. Phys.* **B496** (1997) 177–190, [hep-th/9702038](#).
- [14] M. Bershadsky and C. Vafa, “Global anomalies and geometric engineering of critical theories in six dimensions,” [arXiv:hep-th/9703167](#).
- [15] J. D. Blum and K. A. Intriligator, “Consistency conditions for branes at orbifold singularities,” *Nucl. Phys. B* **506** (1997) 223–235, [arXiv:hep-th/9705030](#).

- [16] P. S. Aspinwall and D. R. Morrison, “Point-like instantons on K3 orbifolds,” *Nucl.Phys.* **B503** (1997) 533–564, [arXiv:hep-th/9705104](#).
- [17] N. Seiberg, “New theories in six dimensions and matrix description of M-theory on T^5 and T^5/Z_2 ,” *Phys. Lett. B* **408** (1997) 98–104, [arXiv:hep-th/9705221](#).
- [18] K. A. Intriligator, “New string theories in six-dimensions via branes at orbifold singularities,” *Adv. Theor. Math. Phys.* **1** (1998) 271–282, [arXiv:hep-th/9708117](#).
- [19] E. Witten, “Phase Transitions in M -theory and F -theory,” *Nucl. Phys.* **B471** (1996) 195–216, [arXiv:hep-th/9603150](#).
- [20] D. R. Morrison and C. Vafa, “Compactifications of F-Theory on Calabi–Yau Threefolds – II,” *Nucl. Phys.* **B476** (1996) 437–469, [arXiv:hep-th/9603161](#).
- [21] D. R. Morrison and W. Taylor, “Classifying bases for 6D F-theory models,” *Centr. Eur. J. Phys.* **10** (2012) 1072–1088, [arXiv:1201.1943 \[hep-th\]](#).
- [22] A. Adams, J. Polchinski, and E. Silverstein, “Don’t Panic! Closed String Tachyons in ALE Spacetimes,” *JHEP* **0110** (2001) 029, [arXiv:hep-th/0108075](#).
- [23] C. Vafa, “Mirror symmetry and closed string tachyon condensation,” [arXiv:hep-th/0111051](#).
- [24] J. R. David, M. Gutperle, M. Headrick, and S. Minwalla, “Closed String Tachyon Condensation on Twisted Circles,” *JHEP* **0202** (2002) 041, [arXiv:hep-th/0111212](#).
- [25] E. J. Martinec and G. W. Moore, “On decay of K theory,” [arXiv:hep-th/0212059](#).
- [26] D. R. Morrison, K. Narayan, and M. R. Plesser, “Localized Tachyons in $\mathbb{C}^3/\mathbb{Z}_N$,” *JHEP* **0408** (2004) 047, [arXiv:hep-th/0406039](#).
- [27] D. R. Morrison and K. Narayan, “On Tachyons, Gauged Linear Sigma Models, and Flip Transitions,” *JHEP* **0502** (2005) 062, [arXiv:hep-th/0412337](#).
- [28] A. Grassi, “On minimal models of elliptic threefolds,” *Math. Ann.* **290** (1991) 287–301.
- [29] P. S. Aspinwall and D. R. Morrison, “Nonsimply connected gauge groups and rational points on elliptic curves,” *JHEP* **9807** (1998) 012, [arXiv:hep-th/9805206](#).
- [30] A. Grassi, J. Halverson, and J. L. Shaneson, “Matter From Geometry Without Resolution,” [arXiv:1306.1832 \[hep-th\]](#).
- [31] D. Mumford, “The topology of normal singularities of an algebraic surface and a criterion for simplicity,” *Inst. Hautes Études Sci. Publ. Math.* **9** (1961) 5–22.

- [32] M. Artin, “Some numerical criteria for contractability of curves on algebraic surfaces,” *Amer. J. Math.* **84** (1962) 485–496.
- [33] H. Grauert, “Über Modifikationen und exzeptionelle analytische Mengen,” *Math. Ann.* **146** (1962) 331–368.
- [34] D. R. Morrison and C. Vafa, “Compactifications of F-Theory on Calabi–Yau Threefolds – I,” *Nucl. Phys.* **B473** (1996) 74–92, [arXiv:hep-th/9602114](#).
- [35] H. W. E. Jung, “Darstellung der Funktionen eines algebraischen Körpers zweier unabhängiger Veränderlicher x, y in der Umgebung einer Stelle $x = a, y = b$,” *J. Reine Angew. Math.* **133** (1908) 289–314.
- [36] F. Hirzebruch, “Über vierdimensionale Riemannsche Flächen mehrdeutiger analytischer Funktionen von zwei komplexen Veränderlichen,” *Math. Ann.* **126** (1953) 1–22.
- [37] O. Riemenschneider, “Deformationen von Quotientensingularitäten (nach zyklischen Gruppen),” *Math. Ann.* **209** (1974) 211–248.
- [38] M. Bershadsky, K. Intriligator, S. Kachru, D. Morrison, V. Sadov, and C. Vafa, “Geometric singularities and enhanced gauge symmetries,” *Nucl. Phys.* **B481** (1996) 215–252, [arXiv:hep-th/9605200](#).
- [39] H. S. M. Coxeter, *Regular complex polytopes*. Cambridge University Press, Cambridge, 1991.
- [40] P. Du Val, *Homographies, quaternions and rotations*. Oxford Mathematical Monographs. Clarendon Press, Oxford, 1964.
- [41] E. Falbel and J. Paupert, “Fundamental domains for finite subgroups in $U(2)$ and configurations of Lagrangians,” *Geom. Dedicata* **109** (2004) 221–238.
- [42] L. B. Anderson, J. J. Heckman, and S. Katz, “T-Branes and Geometry,” [arXiv:1310.1931 \[hep-th\]](#).
- [43] S. Cecotti, C. Cordova, J. J. Heckman, and C. Vafa, “T-Branes and Monodromy,” *JHEP* **07** (2011) 030, [arXiv:1010.5780 \[hep-th\]](#).
- [44] R. Donagi and M. Wijnholt, “Gluing Branes, I,” *JHEP* **05** (2013) 068, [arXiv:1104.2610 \[hep-th\]](#).
- [45] R. Donagi and M. Wijnholt, “Gluing Branes II: Flavour Physics and String Duality,” *JHEP* **05** (2013) 092, [arXiv:1112.4854 \[hep-th\]](#).
- [46] J. J. Heckman and C. Vafa, “An Exceptional Sector for F-theory GUTs,” *Phys. Rev.* **D83** (2011) 026006, [arXiv:1006.5459 \[hep-th\]](#).

- [47] J. J. Heckman, Y. Tachikawa, C. Vafa, and B. Wecht, “ $\mathcal{N} = 1$ SCFTs from Brane Monodromy,” *JHEP* **11** (2010) 132, arXiv:1009.0017 [hep-th].
- [48] J. J. Heckman, C. Vafa, and B. Wecht, “The Conformal Sector of F-theory GUTs,” *JHEP* **07** (2011) 075, arXiv:1103.3287 [hep-th].
- [49] J. J. Heckman and S.-J. Rey, “Baryon and Dark Matter Genesis from Strongly Coupled Strings,” *JHEP* **06** (2011) 120, arXiv:1102.5346 [hep-th].
- [50] R. Miranda, “Smooth models for elliptic threefolds,” in *The birational geometry of degenerations (Cambridge, Mass., 1981)*, vol. 29 of *Progr. Math.*, pp. 85–133. Birkhäuser Boston, 1983.
- [51] A. Grassi and D. R. Morrison, “Anomalies and the Euler characteristic of elliptic Calabi-Yau threefolds,” *Commun. Num. Theor. Phys.* **6** (2012) 51–127, arXiv:1109.0042.
- [52] F. Apruzzi, M. Fazzi, D. Rosa, and A. Tomasiello, “All AdS_7 solutions of type II supergravity,” arXiv:1309.2949 [hep-th].
- [53] M. Artin, “On isolated rational singularities of surfaces,” *Amer. J. Math.* **88** (1966) 129–136.
- [54] O. Zariski, “The theorem of Riemann-Roch for high multiples of an effective divisor on an algebraic surface,” *Ann. of Math. (2)* **76** (1962) 560–615.
- [55] O. J. Ganor, D. R. Morrison, and N. Seiberg, “Branes, Calabi-Yau spaces, and toroidal compactification of the $N=1$ six-dimensional E_8 theory,” *Nucl.Phys.* **B487** (1997) 93–127, arXiv:hep-th/9610251.
- [56] P. C. Argyres and M. R. Douglas, “New phenomena in $SU(3)$ supersymmetric gauge theory,” *Nucl. Phys.* **B448** (1995) 93–126, arXiv:hep-th/9505062.
- [57] D. R. Morrison and W. Taylor, “Toric bases for 6D F-theory models,” *Fortsch. Phys.* **60** (2012) 1187–1216, arXiv:1204.0283 [hep-th].